Pioneering minimum liquid discharge desalination: A pilot study in Lampedusa Island

C. Morgante [a,1], F. Vassallo [a,1], C. Cassaro [a,1], G. Virruso [a,1], D. Diamantidou [b], N. Van Linden [b], A. Trezzi [c], C. Xenogianni [d], R. Ktori [e], M. Rodriguez [e], G. Scelfo [a], S. Randazzo [a], A. Tamburini [a], A. Cipollina [a], G. Micale [a,*], D. Xevgenos [f,*]

[a] Dipartimento di Ingegneria, Università degli Studi di Palermo, - viale delle Scienze Ed.6, 90128 Palermo, Italy
[b] Lenntech BV, Distributieweg 3, 2645, EG, Delfgauw, the Netherlands
[c] Sofinter S.p.A, Piazza Francesco Buffoni, 3, 21013 Gallarate, VA, Italy
[d] Thermossol Steamboilers SA, Tatoiou 94, Acharnes 136 72, Greece
[e] Department of Biotechnology, Delft University of Technology, the Netherlands
[f] Technology, Policy & Management Faculty, Delft University of Technology, the Netherlands

HIGHLIGHTS

- A large-scale MLD plant for seawater valorization is presented (capacity 2.46 m^3/h).
- Energy footprint of the system is reduced, exploiting waste heat from Power Plant.
- In-situ production of chemicals (1 M NaOH, 0.65 M HCl) and high quality freshwater.
- High purity products are recovered: Mg (OH)$_2$ (up to 98 %) and NaCl (>99 %).
- Stability of each unit during the daily operation is successfully accomplished.

GRAPHICAL ABSTRACT
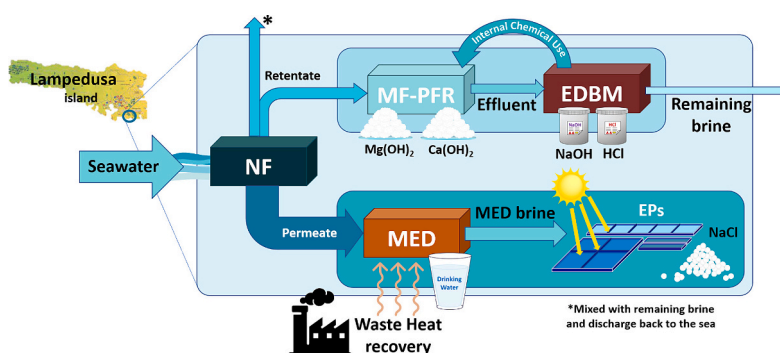
ABSTRACT

Minimum Liquid Discharge (MLD) and Zero Liquid Discharge (ZLD) schemes have been widely proposed in the recent scientific literature not only as a possible solution to brine disposal but also as a non-conventional

Acronyms: AEM, Anionic Exchange Membrane; BC, Brine Concentrator; BCr, Brine Crystallizer; BPM, BiPolar Membrane; CCI, Circular Chemical Inflow; CEM, Cationic Exchange Membrane; Cr, Crystallizer; DPNF, Double Pass NanoFiltration; EC, Electrical Conductivity; ED, ElectroDialysis; EDBM, ElectroDialysis with Bipolar Membranes; Eps, Evaporation Ponds; ESS, Energy Self-Sufficiency; EU, European Union; Ev, Evaporator; FO, Forward Osmosis; HDH, Humidification DeHumidification; HPRO, High Pressure Reverse Osmosis; IEX, Ion Exchange; MCr, Membrane Crystallizer; MD, Membrane Distillation; MED, Multi-Effect Distillation; MFPFR, Multiple Feed Plug Flow Reactor; MLD, Minimum Liquid Discharge; MMF, Multi-Media Filter; MRC, Magnesium Reactive Crystallizer; MSF, Multi Stage Flash; NTC, NaCl Thermal Crystallizer; NF, NanoFiltration; OARO, Osmotic Assisted Reverse Osmosis; PLC, Programmable Logic Control; RE, Resource Efficiency; RED, Reverse ElectroDialysis; RO, Reverse Osmosis; SED, Selective ElectroDialysis; SWRO, Seawater Reverse Osmosis; SCWD, supercritical water desalination; TWP, Total Water Reduction; WAIV, Wind Aided Intensified Evaporation; ZLD, Zero Liquid Discharge.

* Corresponding authors.

E-mail addresses: giorgiod.maria.micale@unipa.it (G. Micale), d.xevgenos@tudelft.nl (D. Xevgenos).

[1] These authors have equally contributed to the activities presented in this work.

sustainable source of raw materials. Nevertheless, very few works have pushed the idea towards a real demonstration activity, and this somehow limits the reliability that such schemes have with respect to the real implementation potential at the industrial scale. In this work, for the first time in the literature, an integrated treatment chain for the sustainable production of freshwater and minerals has been demonstrated at a pre-industrial scale, in the island of Lampedusa (Italy). The treatment chain included a Nanofiltration (NF) step to separate monovalent and bivalent ions, followed by a Multi-Effect Distillation (MED) unit, powered by waste heat from a Thermal Power plant, generating high-quality water (<30 μS/cm) and an ultra-concentrated brine. The latter was treated in Evaporation Ponds (EPs) to generate high purity NaCl (>99 %). On the other side, the NF retentate was treated to selectively recover magnesium and calcium hydroxides (Mg(OH)$_2$ purity up to 98 %) in a novel Multiple Feed-Plug Flow Reactor (MF-PFR). The resulting brine fed an ElectroDialysis with Bipolar Membranes unit (EDBM), generating in-situ alkaline and acidic solutions: chemicals needed for internal usage in the plant. All units were successfully tested, reaching satisfactory performance indicators. Furthermore, the stability of each unit during the daily operational run was assessed and successfully achieved, demonstrating not only the technical feasibility of the proposed demo plant, but also the feasibility of MLD as a sustainable alternative for minerals recovery.

1. Introduction

Many critical issues, apparently considered as a distant matter that only remote future generations would have to face, are nowadays coming across to be more recent than expected. Among them, climate change, water scarcity and land mining depletion are convoying the world economy to adopt a vision of greater sustainability for the future [1]. To tackle freshwater shortage, the last decades have witnessed an exponential increase of desalination plants installed worldwide, reaching >19,000 plants in 2020 [2,3]. However, desalination is necessarily accompanied by brine discharge, having both an economic and environmental impact [4–6].

On the other side, land mining deficiency is becoming a critical matter, with specific respect to several raw materials, for which mining has been characterized by (i) gradual higher costs for both extraction and environmental mitigation [7] and (ii) geographical availability, which places the European Union (EU) in a position of significant dependence from other countries.

To overcome the aforementioned global issues in a sustainable manner, it appears essential to find a "limitless" source for freshwater, on one side, and minerals, on the other, to be exploited with ideally zero environmental impact. A possible solution could be seawater mining, adopting the so-called Minimum Liquid Discharge (MLD)/Zero Liquid Discharge (ZLD) process schemes. To be noted that MLD processes reach a water recovery of 80 %, whilst ZLD processes aim at reaching water recoveries up to 95–99 % [8].

Seawater contains several valuable elements [9]. Some in the highest concentration range are sodium, magnesium, calcium and potassium, which are already commercially extracted as chlorides, sulphates, and carbonates, meanwhile magnesium is usually extracted as hydroxide [10]. Other more valuable elements present in seawater, such as lithium, however are much less concentrated and more difficult to extract [11].

However, the crucial question researchers are trying to answer is: does seawater mining have the necessary elements to fulfil the world economy's dream of sustainability?

Compared to terrestrial mining, seawater mining generally provides several potential advantages: (i) inexhaustible water volumes of the ocean, (ii) constant composition of the oceans' seawater, (iii) the vast capacity of the ocean to dilute treated waste streams and (iv) the stable and fixed footprint of the mining operation [12]. With reference to freshwater/minerals recovery from seawater via an MLD approach, an increasing body of literature is being formed. To the best of the authors' knowledge, all minerals recovery schemes from seawater/desalination brine, that have been proposed in literature heretofore, are reported in Table 1. It is to be noticed how most of these studies are based on conceptual ideas, analyzed from a techno-economic perspective through the use of process modelling and software tools. Among such simulative studies, many process schemes have been proposed by Panagopoulos [13,14]. Firstly, a basic ZLD scheme, comprising Reverse Osmosis (RO),

a Brine Concentrator (BC) and a Brine Crystallizer (BCr), was investigated. Results of an economic analysis showed that 99.36 % water recovery could be achieved with a treatment cost equal to 1.04 $/m^3 of freshwater produced. Variations of the ZLD scheme were analyzed by adding a Forward Osmosis (FO) unit [15] or substituting RO with High Pressure Reverse Osmosis (HPRO) [16] or replacing the BCr with Wind Aided Intensified Vaporation (WAIV) [17]. For all cases, economic feasibility was demonstrated even though such variations had produced slightly lower water recoveries equal to 98.88 %, 99.19 % and 85.75 %, respectively. Furthermore, a new emerging process, called supercritical water desalination (SCWD), is also reported in literature. Van Wyk et al. developed a SCWD lab scale pilot for the production of drinkable water and sodium chloride from seawater, reaching a water recovery of about 91 % and a sodium chloride recovery of 64 % [13]. The same authors carried out a techno-economic analysis on the SCWD technology, showing that the brine treatment cost could be decreased down to 1.16 $/m^3 (with the highest sodium chloride concentration equal to 20 w/w %) [14].

As can be observed in Table 1, many other schemes were suggested but their analysis never continued with an actual implementation in demonstration systems.

The few studies in literature presenting experimental work carried out at bench-scale/laboratory level were mainly limited to the recovery of just water and one salt (i.e., NaCl). Only Tufa et al. [27] attempted to generate energy from seawater brines via a lab-scale membrane-based MD–RED (Membrane Distillation-Reverse ElectroDialysis) system. 92 % freshwater recovery and a gross power density up to 2.4 W/m^2 were achieved. Different was the scope of Zhang et al. [28] who recovered chemicals such as NaOH (85 % pure) and HCl (95 % pure), along with coarse salt (purity of 92 %), integrating chemical precipitation and electro-membrane based technologies.

Even less were the MLD/ZLD schemes implemented at the pilot-scale. Within the framework of the European-funded project SOL-BRINE, a solar-driven evaporator-crystallizer process was developed, recovering 90 % of water and dry mixed salts in Tinos Island (Greece) [30–32]. A large-scale plant was reported by Kieselbach et al. [25] within the framework of the Highcon research project. More precisely, a demonstration plant was constructed comprising RO, NF, ED and MD with a feed capacity of 1.5 m^3/h. Be that as it may, the plant treated a much-diluted feed solution than seawater (pre-treated urban wastewater) recovering NaHCO$_3$ (89.9 % pure) via evaporation and crystallization at lab-scale, thus resulting in a hybrid plant between the lab and pilot scale. Furthermore, a larger demonstration plant was presented by Al-Amoudi et al. [33] in Ummlujj, Saudi Arabia. The plant consisted of an NF unit (feed capacity of 16 m^3/h) for the separation of monovalent and multivalent ions and production of two concentration steps: (i) the first one was made of RO, HPRO +2 stage OARO (Osmotically Assisted Reverse Osmosis) whereas the other step was made of OARO fed by the NF retentate. Overall, freshwater was produced along with two

---

Table 1
Proposed minerals recovery schemes presented in the literature using MLD/ZLD approach exploiting seawater/desalination brine.

Author	Ref.	MLD/ZLD chain*	Salt/water recovery	Conceptual	Lab	Pilot	Additional info
Panagopoulos, 2021 (a), (b)	[15,16]	RO-BC-BCr	• water • mixed salts	✓	–	–	SW Feed capacity = 100 m^3/day Water recovery = 99.36 % Energy consumption = 2240.4 kWh Freshwater cost = 1.04 $/$m^3$
Panagopoulos, 2022 (c)	[17]	RO-FO-BC-BCr	• water • mixed salts	✓	–	–	SW Feed capacity = 100 m^3/day Water recovery = 98.88 % Energy consumption = 1024.6 kWh Freshwater cost = 0.79 $/$m^3$
Panagopoulos, 2022 (d)	[18]	HPRO-BC-BCr	• water • mixed salts	✓	–	–	SW Feed capacity = 100 m^3/day Water recovery = 99.19 % Energy consumption = 2006.2 kWh Freshwater cost = 1.02 $/$m^3$
Panagopoulos, 2022 (e)	[19]	RO-BC-BCr	• water • mixed salts	✓	–	–	SW Feed capacity = 100 m^3/day Water recovery = 85.75 % Energy consumption = 1.3 MWh/m^3 Freshwater cost = 1.01 $/$m^3$
Morgante et al., 2022	[20]	NF-MED-MRC-NTC	• water • $Mg(OH)_2$ • $Ca(OH)_2$ • NaCl	✓	–	–	SW brine Feed capacity = 100 m^3/h Water recovery = 91.01 % Energy consumption = 6.3 kWh/m^3 Freshwater cost = 0.8 €/m^3
El-Zanati et al., 2007	[21]	NF–SWRO–MD	• water	✓	–	–	SW Feed capacity = 100 m^3/d Water recovery = 76.2 % Energy consumption = –– Freshwater cost =0.92 $/$m^3$
Tahir et al., 2022	[22]	MED-HDH-Ev	• water • mixed salts	✓	–	–	MED water production = 1 kg/s HDH water recovery = 40 % ZLD SEC = 720–820 kJ/kg
Poirier et al., 2022	[23]	multi-crystallization system with heat recovery	• water • NaCl • Calcite • Anhydrite • Epsomite	✓	–	–	Brine Feed capacity = 1000 kg/h Water recovery = 99.2 % NaCl recovery = 91.6 % Energy consumption = 60.7 kWh/ton Freshwater cost = 13.79 $/$m^3$
Al Bazedi et al., 2014	[24]	Cr-MCr	• water • NaCl • $MgSO_4$ • $CaCO_3$	✓	–	–	NF brine Feed capacity = 1000 m^3/d Water recovery = 92 % Freshwater cost = 2.82$/$m^3$
Kieselbach et al., 2020	[25]	NF-ED-Ev-Cr-MD	• $NaHCO_3$ • mixed salts	–	✓	✓	Brine Feed capacity = 1.5 m^3/h Water recovery = 65 % Economic analysis for potential larger scale plant: brine disposal cost of 0.5 €/m^3
Von Eiff et al., 2021	[26]	MD-MSF-Cr	• water • Na_2SO_4	✓	✓	–	Water recovery = 89 % Freshwater cost = 0.62 $/$m^3$ Brine treatment cost = 1.24$/$m^3$
Tufa et al., 2015	[27]	MD–RED	• water • energy	–	✓	–	Water recovery = 92 % Gross power density = 2.4 W/m^2
Zhang et al., 2017	[28]	Cr-SED-EDBM	• NaOH • HCl • NaCl	–	✓	–	NaOH (85 % pure) HCl (95 % pure) coarse salt (92 % pure)
Ji et al., 2009	[29]	MD-Cr	• water • NaCl	–	✓	–	Water recovery = 90 % NaCl recovery = 17 kg/m^3
Xevgenos et al. 2014, 2015, 2016	[30–32]	Ev-Cr	• water • dry salts	–	–	✓	Brine Feed capacity = 2 m^3/day 90 % water recovery Powered by solar energy
Van Wyk et al., 2018, 2020	[13,14]	SCWD	• water • dry salts	✓	✓	–	Brine Feed Capacity = 8 kg/h Water recovery = 91 % Brine treatment cost = 1.16$/$m^3$
Al-Amoudi et al., 2023	[33]	NF-(RO-HPRO-2 OARO)-OARO	• multi-valent ion stream • mono-valent ion stream	–	–	✓	Feed capacity = 16 m^3/day Water recovery = 65.2 % No salts are recovered 88.1 kWh/ton NaCl for potential commercial plant

* Refer to Acronyms section for the technologies of each listed MLD/ZLD scheme.

concentrated streams: (i) a monovalent-rich stream with a salinity of 130 g/L and (ii) a bivalent-rich stream with a salinity of 83 g/L. The pilot was then upgraded with more selective NF membranes, a second NF stage and extra stage of OARO. However, no pure salts/minerals were recovered from the concentrated streams.

To the best of the authors' knowledge, there is no study at the moment presenting results from an integrated seawater valorisation treatment system at the demonstration scale that can recover multiple high purity resources contemporarily.

Thus, within the framework of the EU-funded Horizon 2020 project WATER MINING [34–36], this work aims at filling this gap by presenting the results of an integrated system of 5 technologies that:

(i) operates at a large demonstration level, i.e. feed capacity of 2.46 m^3/h;

(ii) is highly versatile, producing both chemicals, high valuable salts (3 useful secondary raw materials) and high quality water;

(iii) exploits waste heat generated by a Power Station, thus reducing the energy footprint of the system.

This project builds on the successful results of the previously funded EU-funded projects SOL-BRINE [30,31] and ZERO BRINE [20]. Building on these previous projects where results from bench-scale or small pilot systems were demonstrated, the WATER-MINING project focused on developing large demo systems that are of pre-industrial scale and relevance.

In the context of areas with limited water and energy sources, the demonstration plant of this work was developed to increase water availability with a sustainable and fully integrated approach. The main aim was to propose and demonstrate a competitive and circular desalination process thanks to:

(i) an option to maximize water production;

(ii) the production of multiple high quality valuable salts;

(iii) a low-energy consumption of the process due to waste heat utilization;

(iv) in-situ chemicals production and internal re-use;

(v) a reduced volume of desalination brine discharged into water bodies.

Such aspects would allow to reduce the overall environmental impact of desalination related to brine discharge and enable a more circular production of resources compared to traditional land-mining within the EU.

2. The sea-mining case study in Lampedusa island (Italy)

The integrated plant was installed in the Sicilian island of Lampedusa (Italy), close to the local Desalination plant and Power station. It comprises 5 different technologies: (i) Nanofiltration (NF), (ii) Magnesium and Calcium Multiple Feed – Plug Flow Reactor (MF-PFR), (iii) ElectroDialysis with Bipolar Membranes (EDBM), (iv) Multi-Effect Distillation (MED) and (v) Evaporation Ponds (EPs). A conceptual scheme of the integrated process is illustrated in Fig. 1.

As can be observed in Fig. 1, seawater was fed to a double pass NF plant, from which two concentrated streams were generated: (i) an NF retentate, rich in divalent ions such as magnesium, calcium and sulphates; and (ii) an NF permeate, rich in monovalent ions such as sodium and chlorides. The NF retentate was sent to the MF-PFR in which, via two consecutive steps at a controlled reaction pH, magnesium and calcium were selectively recovered in the form of hydroxides by adding a sodium hydroxide (NaOH) solution. The clarified effluent of the MF-PFR, free of magnesium and calcium, was then pumped to an EDBM plant in which two chemicals were produced: (i) NaOH solution, that could be used as the alkaline reactant for the MF-PFR, and (ii) HCl solution, that could be used for cleaning purposes within the whole integrated process and in the nearby desalination facility of the island.

The NF permeate valorisation chain integrated more conventional technologies than those present in the retentate one. Firstly, an MED plant exploited the waste heat of the Lampedusa Power plant to produce high quality water. The outlet brine was further sent to a series of evaporation ponds to recover NaCl (table salt grade).

It is worth mentioning that the size of the downstream units following the NF and MED pilots (e.g. MF-PFR, EDBM and EPs) did not match the full capacity required to treat the outlet streams from NF and MED. This was due to practical and financial limitations for the construction of the pilot plants within the project. Nevertheless, the size of all downstream units could be considered fully representative of pre-industrial applications in terms of (i) products characterization, (ii) recovery efficiency and (iii) stability assessment. An integration and circularity assessment of a fully integrated system is, however, reported in the final section of the paper.
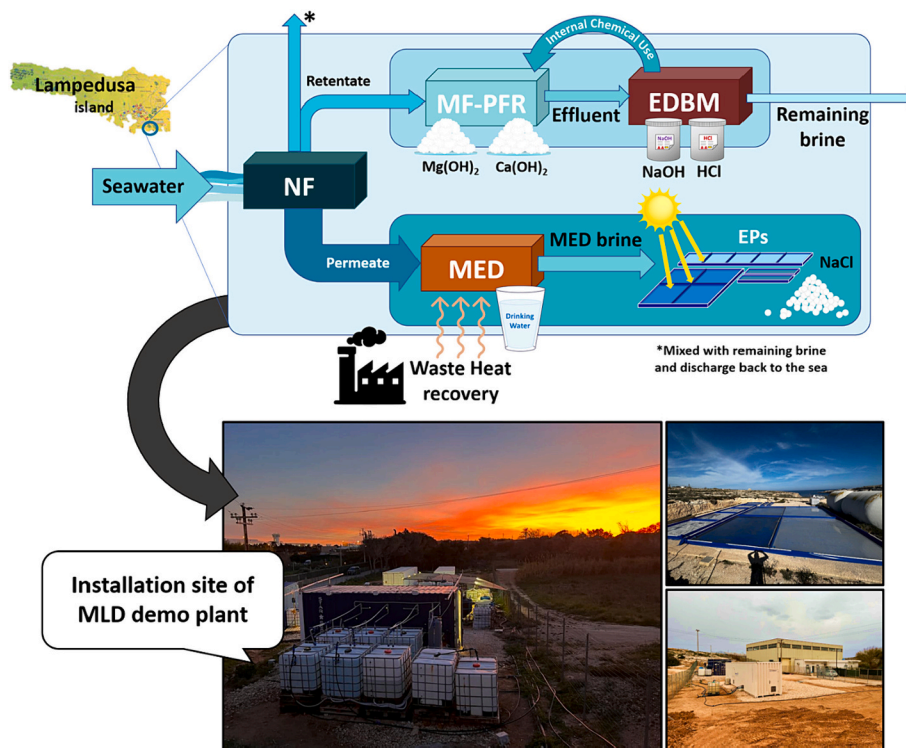

Fig. 1. Conceptual scheme of the seawater valorisation chain in Lampedusa, Italy.

3. Pilot facilities and operational procedure

The single technologies, integrated in the proposed MLD process, were purposely selected to recover valuable resources from the major elements present in seawater. However, to better understand (i) the production efficiency of the overall MLD demonstration plant and (ii) the functioning of each technology, technical details of each pilot unit are reported in the following sections. Performance parameters for each technology are also defined, which were used to evaluate the quality of the recovered products, starting from specific operating conditions for each technology. Such conditions are presented along with the analytical procedure to determine the performance parameters. Finally, 4 specific indicators are introduced to evaluate the circularity of the seawater valorisation chain (in the scenario of a full integration among the units).

3.1. Nanofiltration (NF)

The first technology of the proposed MLD process was Nanofiltration (NF). Starting from a feed stream, the purpose of such pressure-driven membrane-based process is to separate multivalent ions from monovalent ones, thus producing two outlet streams: (i) a permeate stream rich in monovalent ions (i.e., Na^+, K^+, Cl^-) and (ii) a concentrate stream rich in divalent ones (i.e., Mg^{2+}, Ca^{2+}, SO_4^{2-}) [37]. Within the proposed scheme, seawater was taken from a beach well, filtered by a multi-media filter (MMF) for the removal of residual suspended solids and then sent to a Double Pass Nanofiltration (DPNF) system comprising two passes: NF1 and NF2. An image of the pilot plant and a process flow diagram are illustrated in Fig. 2a) and b), respectively.

As can be observed in Fig. 2b), the filtered seawater was subjected to (i) acid (HCl) dosing to decrease the pH and (ii) anti-scalant (AS) dosing (Kurita Vitec 7000) to prevent inorganic scaling on the membrane surface. The dose of the anti-scalant was 1.5 mg/L and 1 mg/L before NF1 and NF2, respectively. High-pressure pumps were used to create sufficient pressure (up to a maximum of 40 bar) to permeate water through the NF1 and NF2 membranes. The two passes of the DPNF system contained 12 and 10 Synder NFX membranes (4040), with a total membrane area of 97 and 81 m^2, respectively. Once dosing occurred, seawater was separated into the NF1 permeate and NF1 concentrate. The NF1 permeate was, in turn, separated into the NF2 permeate and NF2 concentrate. Whilst the NF2 permeate was considered as the final permeate stream, sent to the downstream MED unit, the NF2 concentrate was recirculated back to NF1 and mixed with seawater to form the NF1 feed. The NF1 retentate, conversely, was sent to the MF-PFR pilot in order to be valorized.

Overall, the DPNF system treated a feed flow rate of 2.46 m^3/h with a total permeate recovery of 69 %. Hence, the NF2 permeate had a flow rate of 1.70 m^3/h, whereas the NF1 concentrate had a flow rate of 0.76 m^3/h. Finally, to allow automatic and continuous operation and data logging, the DPNF system was equipped with pressure transmitters, flow transmitters, electrical conductivity (EC) sensors, temperature sensors, pH sensor and electrical valves.

To demonstrate the performance and stability of the DPNF plant, the following performance parameters were determined and logged throughout the operation:

- Permeate recovery $R_{p,(s.p\ or\ DPNF)}$ of single pass (or DPNF plant), which represents the quantity of permeate of the single pass (or NF2) produced with respect to the feed solution of the single pass (or global feed solution), calculated according to Eq. (1):

$$R_{p,(s.p\ or\ DPNF)} = \frac{Q_{p,(s.p\ or\ NF2)}}{Q_{f,(s.p\ or\ DPNF)}} \times 100 \tag{1}$$

where $R_{p,(s.p\ or\ DPNF)}$ is the permeate recovery of the single pass (or DPNF plant) [%], $Q_{p,(s.p\ or\ NF2)}$ is the permeate flow rate of the single pass (or NF2) [m^3/h] and $Q_{f,(s.p\ or\ DPNF)}$ is the feed flow rate of the single pass (or the DPNF plant) [m^3/h].

- Ionic rejection $r_{i,(s.p\ or\ DPNF)}$ of the single pass (or DPNF plant) calculated as the difference of ion concentration between the feed of the single pass (or DPNF plant) and the permeate of the single pass (or NF2) divided by the concentration of the ion in the feed solution of the single pass (or DPNF plant) (see Eq. (2)).

$$r_{i,(s.p\ or\ DPNF)} = \frac{C_{i,f,(s.p\ or\ DPNF)} - C_{i,p,(s.p\ or\ DPNF)}}{C_{i,f,(s.p\ or\ DPNF)}} \times 100 \tag{2}$$

where $r_{i,(s.p\ or\ DPNF)}$ is the ionic rejection [%] of ion i concerning the single pass (or DPNF plant), $C_{i,f,(s.p\ or\ DPNF)}$ is the feed ion concentration of the single pass (or DPNF plant) [mg/L] and $C_{i,p,(s.p\ or\ DPNF)}$ is the permeate ion concentration of the single pass (or NF2) [mg/L].

- Membrane permeability K, computed as the permeate flow rate divided by transmembrane area and transmembrane pressure (Eq. (3)):

$$K = \frac{Q_{p,NFn}/A_{m,NFn}}{TMP} \tag{3}$$

where K is the membrane permeability [L/m^2/h/bar], $Q_{p,NFn}$ is the permeate flow rate of NF1 or NF2 [m^3/h], $A_{m,NFn}$ is the membrane area of NF1 or NF2 [m^2] and TMP is the trans-membrane pressure of NF1 or NF2 [bar].

3.2. Multiple Feed – Plug Flow Reactor (MF-PFR)

The first stage of the NF retentate valorisation line was the Multiple Feed – Plug Flow Reactor (MF-PFR): a selective reactive crystallization process to recover Magnesium and Calcium in the form of hydroxides via the addition of an alkaline reactant (NaOH solution), at a controlled
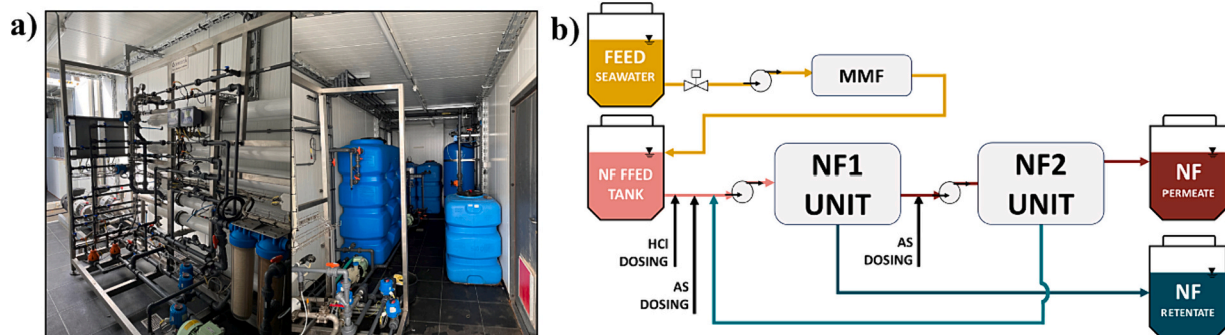

Fig. 2,. a) Image of the NF pilot plant; b) Process flow diagram of the NF unit adopted.

reaction pH. The pilot plant consisted of (i) a patented reactive crystallizer [38,39], accompanied by (ii) a drum filter for the recovery of solids and (iii) a neutralization step to neutralize the final clarified solution, suitable for feeding the EDBM unit. An image of the pilot plant and a schematic representation of the Mg and Ca recovery process is shown in Fig. 3 a) and b), respectively.

The core of the pilot was the reactor, in which the feed solution (DPNF retentate) was directly mixed with a NaOH solution via multiple nozzles placed along the entire length of a cylindrical vessel, containing the alkaline reactant. The position and orientation of the nozzles were such that they promoted fast mixing of both reactants. Moreover, as shown by the study previously conducted by Morgante et al. [40], a recycling loop of the outlet slurry had to be adopted, allowing to achieve a Magnesium Hydroxide (Mg(OH)$_2$) slurry, easy to settle and filter. Mg(OH)$_2$ precipitation occurs at pH 10.6 whereas Calcium Hydroxide (Ca(OH)$_2$) at pH 13. Therefore, it was essential to monitor the conductivity of the feed solutions, the reaction pH and reactant solution flow rates via sensors (KROHNE). To guarantee the operation at a specific pH value (and therefore promote either Mg or Ca precipitation), the feed flow rates were controlled via a PLC implemented in LabVIEW® environment.

Following the precipitation of Mg(OH)$_2$ (1° precipitation step), the produced slurry was sent to a settling tank. The resulting clarified solution was pumped to an inter-stage tank to be further treated by the MF-PFR to recover Ca(OH)$_2$ (2° precipitation step), whilst the concentrated slurry was sent to the filtration step.

Following the second precipitation step, where Ca(OH)$_2$ precipitated at reaction pH of 13, the resulting slurry was sent to a different settling tank. The concentrated slurry was pumped to the drum filter, whilst the final clarified solution was treated in a neutralization step via HCl dosing. The neutralized brine pH was monitored via an in-line pH-meter (KROHNE, PH8320).

A semi-industrial scale drum filter was employed to recover magnesium hydroxide and calcium hydroxide from their respective concentrated slurries. Technical details of the filtration section have been previously provided by Vassallo et al. [39].

To assess the production efficiency and the quality of products achieved by the MF-PFR unit, two performance indicators were taken into consideration:

- Recovery, which indicates the total amount of magnesium (or calcium) recovered with respect to the total amount of magnesium (or calcium) present in the feed solution (calculated according to Eq. (4)).

$$R_j = \frac{n_j^{\circ} - n_j}{n_j^{\circ}} \times 100 \tag{4}$$

where n is the molar flow-rate [mol/min], the apex $^{\circ}$ refers to the inlet molar flow rate, while the subscript j refers to a specific cation (i.e. magnesium).

- Purity of solid, calculated as the amount of magnesium (or calcium), with respect to the total amount of cations measured via Ionic Chromatography (IC) or titration (see Eq. (5)).

$$Purity_{Mg^{2+}\left(or\ Ca^{2+}\right)} = \frac{C_{Mg^{2+}(or\ Ca^{2+})}}{\sum_{i=1}^{n} C_i} \times 100 \tag{5}$$

where C_i is the molar concentration [mol/L] of the ith ion.

3.3. ElectroDialysis with Bipolar Membranes (EDBM)

The neutralized effluent from the MF-PFR was eventually sent to the Electrodialysis with bipolar membranes (EDBM) unit. EDBM is an electro-membrane process, which allows the production of chemical reagents, such as acid and base, starting from saline solution and electrical energy [41,42]. This technology foresees the use of three types of ion exchange membranes (IEXs) named cationic (CEM), anionic (AEM) and bipolar membrane (BPM). In particular, the latter is composed of a cationic and an anionic membrane, welded together. The sequence of a CEM, an AEM and a BPM represents the repeating unit of this equipment, also called triplet. Applying an electric field through the cell pack, the cations migrate towards the cathode (the negative electrode) while the anions migrate towards the anode (the positive cathode). Once migrated, the cations encounter the hydroxyl ions (coming from the BPMs) producing a base solution. As for the anions, the interaction with protons (from BPMs) produces an acidic solution. In the pilot a large scale EDBM stack was employed to produce specifically sodium hydroxide (NaOH) and hydrochloric acid (HCl). The pilot plant was composed by two main parts: the EDBM stack and the pumping station and measuring/control instruments, as can be observed in Fig. 4a).

The EDBM stack (FuMA-Tech GmbH, model: FT-ED1600–3) was composed of 40 triplets divided into two parts of 20 triplets each
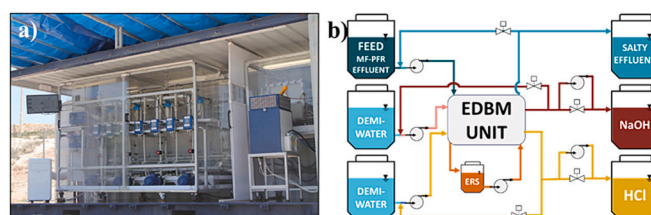

Fig. 4. a) Image of the EDBM pilot plant (pumping station and measuring/control instruments on the left, DC drive and EDBM stack on the right); b) Process flow diagram of the Feed&Bleed configuration adopted.
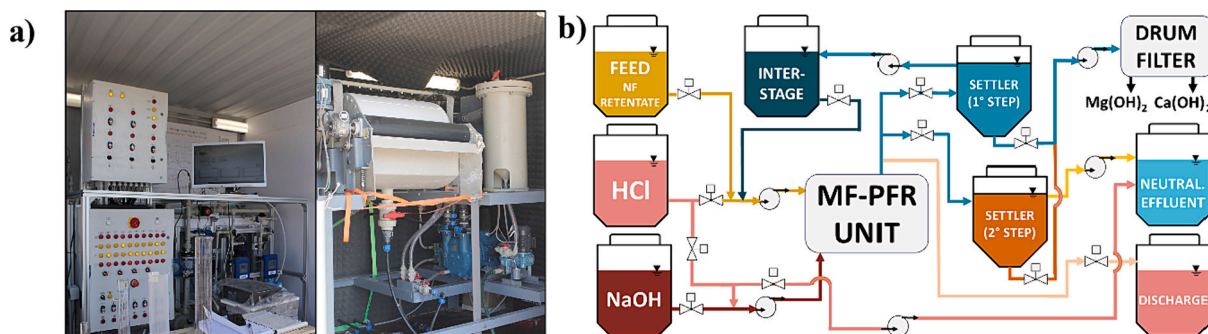

Fig. 3. a) Image of the MF-PFR (left) and Drum filter (right) pilot plants; b) Process flow diagram of the Mg/Ca precipitation process implemented within the MF-PFR pilot plant.

reaching a total membrane area of 19.2 m². The unit was provided with the following ionic exchange membranes (IEXs): FUMASEP® FAB-PK anion exchange membranes (PET reinforced with PK, 130 μm thick,), FUMASEP® FKB cation exchange membranes (PK reinforced with PK, 130 μm thick), and FUMASEP® FBM bipolar membranes (composite membrane reinforced with woven PEEK, c. 160 μm thick). The anode and cathode were DSA and stainless steel, respectively. As far as the hydraulic circuit is concerned, four lines were designed, one for each electrolytic solution (see Fig. 4b)). Magnetic flowmeters, conductivity meters, pH meters and pressure transducers were installed to monitor the main variables involved in the process. To control the latter and for data acquisition purposes, National Instrument® hardware and Lab-VIEW software were used. Further technical details on the EDBM pilot plant design and construction are reported in [43].

The EDBM unit operated in a continuous mode adopting a Feed&-Bleed configuration (as depicted in Fig. 4b)). This allowed to achieve different product targets varying the outlet flowrate of acid and base streams, thus satisfying several concentration requirements.

To analyze the performance of the EDBM unit, two main indicators were employed:

- Current efficiency (CE, %), which accounts for the amount of electric charges introduced into the system successfully converted into the production of protons or hydroxide ions (calculated according to Eq. (6)):

$$CE = \frac{Q_{p,out}\left(C_{p,out} - C_{p,in}\right)F}{60\, N_{tr}\, i\, A_m} \times 100 \tag{6}$$

Where $Q_{p,out}$ is the outlet flowrate of product [L/min], $C_{p,out}$ and $C_{p,in}$ are the outlet and the inlet product concentration [mol/L], respectively, F is Faraday's constant (i.e., 96,485 C/mol), N_{tr} is the triplet number, A_m is the membrane active area [m²] and i [A/m²] is the electric current density provided to the stack.

- Specific Energy Consumption (SEC) [kWh/kg], which is the energy consumed to produce 1 kg of the desired product (calculated according to Eq. (7)):

$$SEC = \frac{U\, i\, A_m}{60\, Q_{p,out}\left(C_{p,out} - C_{p,in}\right) M_p} \tag{7}$$

Where U is the electric potential (V) applied to the stack, and M_p is the molecular weight of the desired product [g/mol].

3.4. Multi-Effect Distillation (MED)

As for the NF permeate valorisation chain, the first step consisted in a Multi-Effect Distillation (MED) unit. MED is a thermal-based process exploiting a heat source to produce high quality water by evaporating saline solutions (i.e., seawater) [44,45]. Such process takes place inside evaporative chambers called effects, each one presenting a heat transfer surface across which heat is exchanged between the raw water and a condensing steam. The primary steam comes from a hot source at a temperature typically below 100 °C under saturation conditions. Whilst condensing, it releases its latent heat promoting the evaporation of the raw water. Such condensation-evaporation process is maintained effect-by-effect due to a different saturation condition of the two streams guaranteed by the presence of a vacuum system (i.e., vacuum pumps or steam ejectors) and a decreasing pressure profile along the effects. Two streams are generated from the initial raw water: (i) vapour (secondary steam) and (ii) concentrated water (brine). The produced steam acts as the "hot source" for the following evaporation effect to then be condensed by exchanging heat with raw water at a lower temperature (and pressure). As for the brine, this also flows to the next effect, joining the newly produced brine. The same process is repeated along all the effects of the evaporator. Operating in such manner, the thermal energy

recovery of the unit is maximized. The vapour generated in the last effect is condensed in a final condenser, where all distillate streams are merged into a single stream. Also the several concentrated brine streams produced in each effect are merged into a single stream to be generally discharged.

Within the process scheme, the MED pilot unit was operated feeding the NF permeate, producing (i) high quality water and (ii) ultra-concentrated brine, which was directed to the solar evaporating ponds for NaCl recovery. A picture of the installed MED plant and the process flow diagram of the pilot unit can be observed in Fig. 5a) and b).

More specifically, the pilot installed in Lampedusa consisted of:

(i) A heat input section (steam generation section), arranged as a closed loop circuit of demineralized water to produce "primary steam". Via a heat exchanger, "waste" heat was recovered from the cooling circuit of the power plant and transferred to a secondary stream of demineralized water. This stream was conveyed into a drum where the vapour was produced by flash;

(ii) A heat recovery section (MED evaporator), where the heat input was provided by the heat exchange in every effect, producing distilled water;

(iii) A heat reject section (final condenser), where the thermal energy was finally released at lower temperature (condenser) to a cooling water circuit, thus closing the heat balance;

(iv) Auxiliary systems (vacuum generation unit and chemicals dosing unit).

The following operating/performance parameters were used in order to assess the system behavior:

- Concentration Factor (CF): indicating the molar concentration of sodium chloride (equivalent) in the outlet brine divided by the concentration in the inlet one.

$$CF = \frac{C_{NaCl,out,brine}}{C_{NaCl,in,brine}} \tag{8}$$

Where $C_{NaCl,out,brine}$ is the brine outlet molar concentration of NaCl [mol/L] and $C_{NaCl,in,brine}$ is the brine inlet molar concentration of NaCl [mol/L].

- "Specific Electric Energy Consumption" (SEEC): expressing the electrical energy consumption per cubic meter of produced distilled water, computed as the ratio between the electrical energy and the total amount of distilled water:

$$SEEC = \frac{Power_{el}}{\dot{m}_{dist}} \tag{9}$$

- Gain Output Ratio (GOR): indicating the conversion of primary vapour into distillate water. It is computed as the ratio between the mass flowrate of produced distillate $\dot{m}_{dist}$ [kg/h] and mass flowrate of the produced primary vapour $\dot{m}_{steam}$ [kg/h]:

$$GOR_{gross} = \frac{\dot{m}_{dist}}{\dot{m}_{steam}} \tag{10}$$

3.5. Evaporative ponds (EPs)

At the end of the treatment chain, Evaporative Ponds (EPs) were built to recover pure Sodium Chloride (NaCl), mimicking the conventional process of natural saltworks, producing table-salt by fractional precipitation in several shallow basins. An image of the ponds along with a schematic diagram are shown in Fig. 6a) and b), respectively. They were built using wood planks for the border and a cloth in PVC covering a layer of sand placed on the concrete platform. A depth of 10 cm was adopted as computed during the design phase.

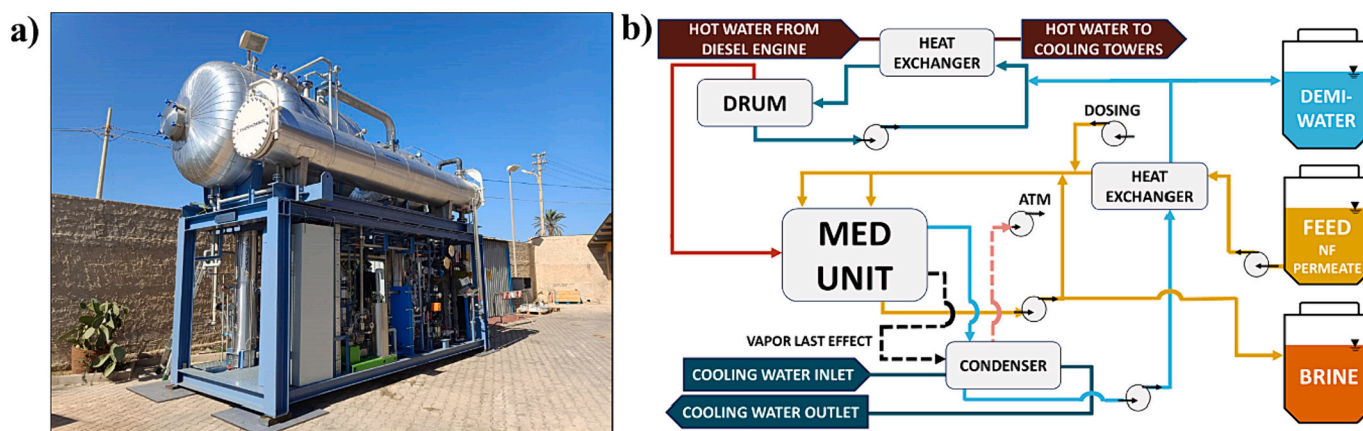In detail, Pond A, divided into four smaller ponds, was designed as

Fig. 5. a) Picture of the MED pilot plant; b) Process flow diagram of the MED unit.
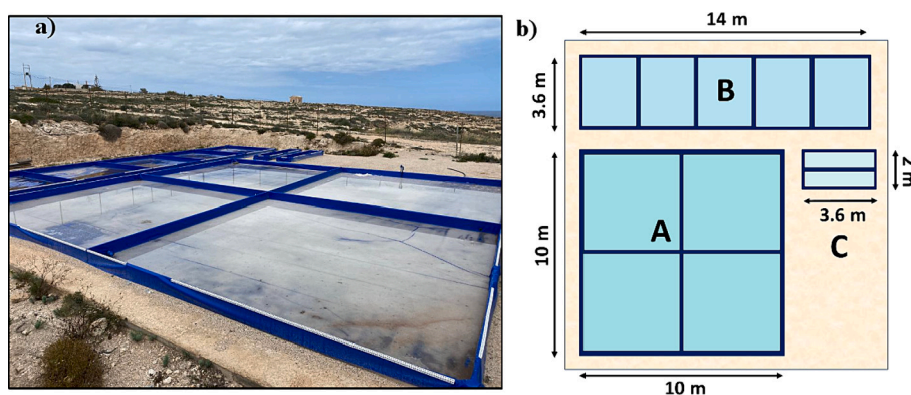

Fig. 6. a) Image of Evaporation Ponds; b) Footprint of the evaporation ponds employed.

the "hot" pond where the outlet solution exiting the MED unit was collected. In this pond, the NaCl concentration increased up to the saturation point of NaCl. Pond B, divided into six smaller ponds, represents the "crystallizing" pond where the NaCl solid crystals precipitated. Finally, Pond C, divided into two smaller ones, allowed to collect the exhausted solution, i.e. the final exhausted bittern. For the design of the ponds and the choice of the inlet/outlet brine flow rates, (i) the Penman equation was used to estimate the evaporation rate [46] and (ii) PHREEQC software using the Pitzer thermodynamic package was employed to simulate the salt precipitation [47].

In detail, the evaporation rate E (mm/day) was estimated on the basis of a value of the net solar radiation calculated by a correlation developed by ENEA, the Italian "National Agency for New Technologies, Energy and Sustainable Economic Development" [48]. A value of 25 MJ/m^2/day was assumed for May, considering the geographical coordinates of Lampedusa. The other parameters were assumed as the following: wind speed 5 m/s, humidity 77 % and temperature 19.7 °C.

The results of the design are shown in Table 2, where the

composition and flow rates from/to each pond are listed. Of course, values for the outlet of pond A are the inlet for pond B and the same applies for the outlet from pond B and the inlet for pond C.

The purity of NaCl was calculated as the amount of sodium (as sodium chloride) with respect to the total amount of salts in the samples. All the species present in the samples were detected via Ionic Chromatography (IC) analysis. The purity was calculated according to the following equation:

$$Purity_{NaCl} = \frac{M_{NaCl_{real}}}{M_{salt}} \times 100 \tag{11}$$

where $M_{NaCl_{real}}$ is the measured mass of NaCl in the solid sample and M_{salt} is the total salt mass.

3.6. Operating conditions and analytical procedure

The technologies comprising the proposed MLD process scheme functioned according to the operating conditions reported in Table 3 (main flow rates) and Table 4 (inlet composition), including specific parameters of each technology. As it is possible to observe from Table 2, the recovery of NF1 and NF2 was fixed at 71 % and 92 %, respectively, in order to reach a permeate flow rate equal to 1.70 m^3/h and a retentate flow rate equal to 0.76 m^3/h. The NF plant typically operated for 8 h per day and daily samples of the feed, NF1 retentate and NF2 permeate were collected. As far as the MF-PFR is concerned, the pilot unit presented a much smaller scale than the NF, as can be noted by its flow rates reported in Table 2. Furthermore, employing a 1 mol/L NaOH solution received from the EDBM unit, it was necessary to adopt a NaOH flow rate of 0.85 L/min and 1 L/min for the 1° and 2° precipitation steps, respectively, in order to reach a pH = 10.6 for Mg(OH)$_2$ precipitation

Table 2
Inlet mean ions composition in the ponds.

	Inlet Composition [g/L]							Flow rate,IN (L/h)
	Na$^+$	K$^+$	Ca^{2+}	Mg^{2+}	Cl$^-$	TDS	NaCl	
Pond A	69.5	2.102	0.13	0.13	125	197	177	180
Pond B	123	3.55	0.24	0.24	194	321	311	147
Pond C	101	45.9	3.07	3.07	211	367	253	117

Table 3

Main flow rates and specific operating parameters of each technology comprising the proposed MLD process.

Technology	Stream	Flow rate	Additional specific parameters
NF	Feed	2.46 m^3/h	NF1 recovery = 71 %
	Permeate	1.7 m^3/h	NF2 recovery = 92 %
	Retentate	0.76 m^3/h	
MF-PFR	1° Brine	2.5 L/min	1° step pH = 10.6
	1° Alkaline	0.85 L/min	2° step pH = 13
	2° Brine	1.5 L/min	C_{NaOH} (1° step) = 1 mol/L
	2° Alkaline	1 L/min	C_{NaOH} (2° step) = 1 mol/L
			Total Capacity Mg(OH)$_2$ = 14.4 ton/y
EDBM	Salt	1.8 L/min	Current density = 400 A/m^2
	Acid	1.35 L/min	Voltage = 55 V
	Base	1.1 L/min	C_{ERS} = 0.25 mol/L
	ERS	20 L/min	H$_2$O employed as feed for acid and base channels
			Total Capacity NaOH = 21.23 ton/y
			Total Capacity HCl = 15–16 ton/y
MED	Feed	1.75 m^3/h	Pressure condenser = 70 mbar
	Distillate	1.5–1.6 m^3/h	Heat source T* = 80 °C
	Rec. Brine	6.5 m^3/h	Cooling water T = 20 °C
	Cooling water	20 m^3/h	
	Brine	0.2–0.3 m^3/h	
EPs	Feed	180 L/h	–

* The heat source supplied into MED was cooling water coming from a diesel engine used as a power generator.

and pH = 13 for Ca(OH)$_2$ precipitation. The MF-PFR also operated for 8 h per day for the 1st step (whereas 5 h per day for the 2nd step) and samples of the Mg(OH)$_2$ and Ca(OH)$_2$ slurry were collected. As for the operation of the EDBM, the scale of the pilot was similar to that of the MF-PFR. A current density of 400 A/m^2 was adopted with an applied voltage equal to 55 V to guarantee a sufficient production rate of the alkaline stream. Moreover, a 0.25 mol/L Na$_2$SO$_4$ solution was used as the ERS solution for the electrodes of the EDBM stack. The acid and base compartments were fed with a permeate from a Seawater Reverse Osmosis (conductivity of 400 μS/cm) operating within the power station of the island to produce industrial water. During the 5 h operation per day, samples of the acid and base solutions were collected typically once or twice.

The operation of the MED pilot plant was conducted similarly to the other plants, although its operation also depended on several parameters concerning the availability and temperature of its utilities (mainly the hot water coming from the cooling circuit of a diesel engine).

The pressure in the condenser, which determines the operating pressure in the distillation effects, was typically fixed at 70 mbar. The (estimated, not measured) hot water flow rate was 25 m^3/h and this was generally available at an average temperature of 80 °C with fluctuations of ±5 °C.

The cooling water used as the cold utility was available at an average temperature of 25 °C. In this case, however, the thermal power subtracted from the condenser was variable by varying the input flow and was used to adjust the final condenser pressure. Samples of produced distillate and brine were taken during the 4 operating hours per day of the MED unit to be subsequently analyzed.

Finally, the brine recirculation flow rate was fixed at a value of 6.5 m^3/h, to (i) ensure effective wettability of the tube bundle even at low feed flow rates and (ii) guarantee an adequate residence time inside the

MED, greatly concentrating the brine.

For the evaporation ponds, the feed flow rate was nominally fixed to 180 L/h, operating in semi-batch. The crystallized product was collected for purity analyses.

Concerning the analysis of all the aqueous samples:

- the concentration of Na$^+$, K$^+$, Ca^{2+}, Mg^{2+} and SO$_4^{2-}$ were measured by Inductively coupled plasma-optical emission spectrometry (ICP-OES) or Ion Chromatography analysis (Metrohm 882 Compact Ion Chromatography);
- the Cl$^-$ concentration was measured by discrete Skalar analyses
- the HCO$_3^-$ concentration was measured via titration.

As for the determination of the purity of the recovered solids, a precise procedure was adopted. The wet solid was filtered and washed with demineralized water (for Mg(OH)$_2$ and Ca(OH)$_2$) or with a saturated NaCl solution (for NaCl). Then, a weighed quantity was dried in an oven at 120 °C for 24 h and, after cooling to room temperature, the detection of the weight was repeated to estimate the initial humidity content. To analyze the concentration of anions and cations in the solid, the dried sample was dissolved in deionized water and analyzed by Ionic Chromatography (IC) via a Metrohm 882 Compact IC equipped with the anion-exchange Metrosep® A Supp 5 and a cation-exchange Metrosep® C4 columns. The mobile phase for the anions detection was a solution of Na$_2$CO$_3$ 3.2 mM and NaHCO$_3$ 1 mM fluxed at 0.7 mL/min, whereas the one for cations was a 5.5 mmol/L H$_3$PO$_4$ solution.

3.7. Circularity assessment

After the assessment of the technical feasibility and stability of the system, it was essential to identify circular opportunities and linear risks

Table 4

Inlet composition of each technology comprising the proposed MLD process.

Technology	Inlet Composition						
	[mg/L]						
	Na$^+$	K$^+$	Ca^{2+}	Mg^{2+}	Cl$^-$	SO$_4^{2-}$	HCO$_3^-$
NF	12,960	438	425	1300	21,090	3230	183
MF-PFR	15,590	669	1400	4650	30,565	10,460	315
EDBM	17,000	303	–	–	19,600	5010	2730
MED	11,100	423	15	12	17,143	5	79
EPs	69,510	2102	219	94	110,126	0	–

to enhance durability and resilience. For this purpose, the following indicators were formulated. To assess the circularity of the system, first, it was necessary to indicate the waste reduction achieved in the system due to the circularity measures. In this work, the brine reduction of the proposed circular system compared to the linear RO desalination plant was measured. The Total Waste Reduction (TWP) [49] was estimated according to the following equation:

$$TWP = \frac{Volume\ of\ SWRO\ brine\ (non\ circular)\left[\frac{m^3}{h}\right] - Volume\ of\ brine\ from\ a\ circular\ system\left[\frac{m^3}{h}\right]}{Volume\ of\ SWRO\ brine\ (non\ circular)\left[\frac{m^3}{h}\right]} \times 100 \tag{12}$$

Where the volume of SWRO brine (non-circular) was estimated based on 40 % efficiency assumption for the RO plant. The volume of brine from the circular system was considered to be the outlet salt stream from the EDBM unit.

Resource efficiency (RE) [50] showed the efficiency of recovery of valuable products from seawater in the context of circular economy. RE was defined as the ratio of useful material output and input and was estimated according to the following equation:

$$RE = \frac{Mass\ of\ useful\ materials\ output\left[\frac{kg}{h}\right]}{Mass\ of\ useful\ materials\ input\left[\frac{kg}{h}\right]} \times 100 \tag{13}$$

Since the capacity of each unit was different, the RE was assessed for each product based on the capacity of the required technology.

Regarding the circularity of resources, the required chemicals and water were produced internally from seawater brine. Circular Chemical Inflow (CCI) [51] assessed the circularity of chemicals used in the process, specifically HCl and NaOH. CCI was estimated according to the following equation:

$$CCI = 1 - \frac{Volume\ of\ chemical\ inflow\ from\ non\ circular\ sources\left[\frac{m^3}{h}\right]}{Total\ volume\ of\ chemical\ inflow\ (circular\ and\ non\ circular)\left[\frac{m^3}{h}\right]} \times 100 \tag{14}$$

Where the volume of chemical inflow from circular and non-circular sources referred to HCl and NaOH that were used in MF-PFR unit.

Finally, the proposed system aimed at low-energy consumption due to waste heat utilization. Waste heat was used to provide the thermal energy requirements in the MED unit and solar energy to recover NaCl salt from the evaporation ponds. Therefore, it was important to measure the energy self-sufficiency of the system. The Energy Self-Sufficiency (ESS) [51] was estimated according to the following equation:

$$ESS = \frac{Sustainable\ Energy\ in\ kWh\ produced\ and\ utilised\ on\ site}{Total\ energy\ demand\ of\ the\ system\ [kWh]} \times 100 \tag{15}$$

Where thermal energy requirements were translated to electricity requirements assuming that the efficiency of the diesel engine was 30 % based on the fuel.

4. Results and discussion

The overall technical feasibility of the proposed pilot scale MLD chain was evaluated via (i) the analysis of the collected samples of each recovered product and (ii) the calculation of specific performance indicators, previously mentioned for each pilot plant comprising the

chain. Furthermore, to demonstrate the robustness of the proposed treatment chain in achieving products with constant specific characteristics, the stability of the main operating parameters of each technology was investigated during their daily operational run. It is worth mentioning that each unit was operated for a different amount of hours, due to the different nominal capacity of each of the pilot units, which in fact required the installation of buffer tanks in order to interconnect the different units and fully operate the integrated chain. Finally, results of the integration and circularity assessment were reported.

4.1. DPNF pre-treatment stage performances

It is widely known in literature that the performances of the pre-treatment step (in our case, the DPNF) of any seawater/brine mining scheme are crucial to the overall performance of the entire process [12], due to its ability of producing water streams with suitable features to be further processed (selectively rich in monovalent or bivalent ions, in our case). A subsequent advantage of such ability would be to successfully recover resources with high purity (and recovery) via downstream crystallization steps. Thus, it was necessary to investigate the DPNF capacity of selectively separating ions. As can be observed in Fig. 7, results showed that the DPNF process allowed >97 % rejection of the multivalent ions. More specifically, 97 %, 99 % and 100 % were the rejection values achieved for Ca^{2+}, Mg^{2+} and SO_4^{2-}, respectively. In contrast to the high multivalent ion rejection, the monovalent ions Na^+, K^+ and Cl^- were only limitedly rejected: 14 %, 3 % and 19 %, respectively. Based on the results, the DPNF process proved to be effective in separating monovalent and multivalent ions, originally present in seawater.
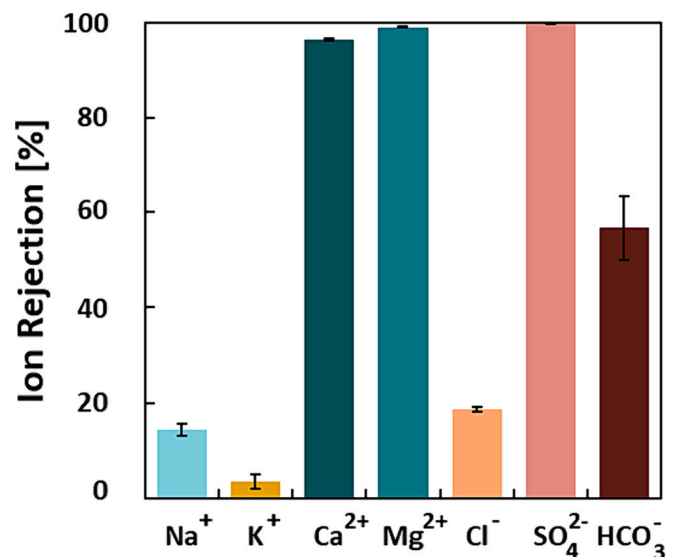

Fig. 7. The ions rejections of the DPNF process (average values are presented, whereas the error bars show the deviation for the minimum and maximum values, considering two measurements).
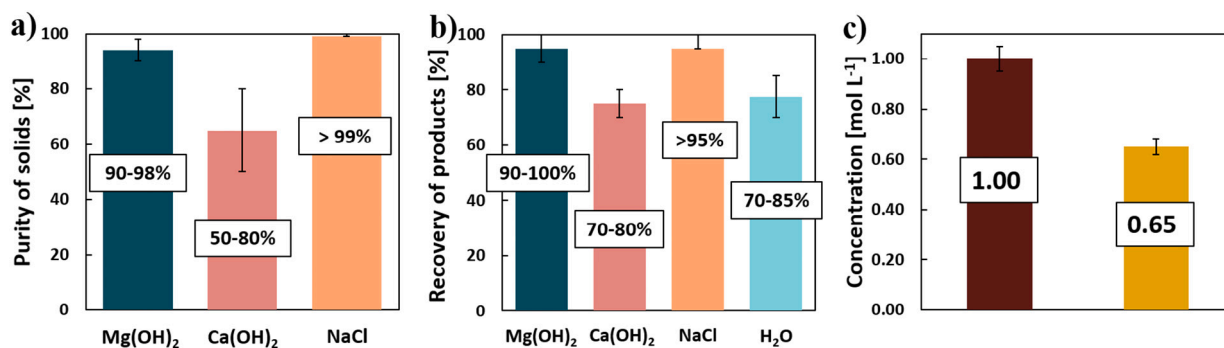
Fig. 8. a) Purity of recovered solids; b) Recovery of solids and H$_2$O (MED distillate); c) Concentration of chemicals produced by the EDBM unit. The average value is reported, with error bars indicating the variability of each parameter along the pilot experimental campaign. Concentration of the chemical was computed by acid-base titration.

4.2. Purity and recovery of products/chemicals

The brine valorisation lines, treating the DPNF retentate and the MED brine produce a number of products, starting from Mg(OH)$_2$ and a Ca(OH)$_2$ and Mg(OH)$_2$ mixture (in the second precipitation step), passing through the chemicals generated in the EDBM up to the high purity NaCl crystallized in the evaporative ponds. Purities of such products changed depending on the tested operating conditions, but Fig. 8a) reports the purity of all the recovered solids as an average of measured purities during the experimental assessment of each single technology. On the other side, Fig. 8 b) and c) report the recovery of each product and the concentration of the acid/alkaline streams produced, respectively. It is worth mentioning that such values changed with variable operating conditions during the experimental campaign, for each experiment a couple of samples were taken when the stationary condition was achieved. Thus, an average value is reported with error bars indicating the variability of each parameter.

Results of the analyses of the products showed that the MF-PFR was able to produce Mg(OH)$_2$ with an average purity around 94 %. As described in two previous works by Vassallo et al. [39,52], the purity of magnesium hydroxide was affected by the presence of carbonate/bicarbonate in the feed, causing the co-precipitation of calcium as calcium carbonate, which was the most insoluble species at the operating conditions of the MF-PFR (pH about 10.6 and 20–25 °C). In addition, the recovery of such hydroxide during the 1st precipitation step was high, reaching values >90 %. Attempts to increase the recovery can be made by increasing the outlet pH via the increase of the alkaline flow rate.

As for the 2nd precipitation step, aiming at the removal of all bivalent cations (magnesium and calcium), the IC analysis of the solid showed that the purity of Ca(OH)$_2$ was in average >60 %. The purity was affected by the co-precipitation of magnesium in the form of hydroxide caused by the incomplete removal of magnesium during the 1st step of precipitation. Calcium removal efficiency was about 70–80 %, while magnesium was totally precipitated, due to the high pH reached (about 13).

Excellent results were also obtained for the NaCl produced via evaporation ponds. NaCl purity >99 % was achieved, well above the minimum required purity limit for food applications (97 %) [53]. Its

recovery was above 95 %, as can be observed in Fig. 8 b).

In particular, four samples were withdrawn from four of the subponds obtaining an average value for the NaCl purity of 99.1 % obtained via IC.

High freshwater recovery was also achieved by the MED unit, reaching values up to 85 % (considering the single MED unit, which achieved concentration factors in the brine up to 7).

Finally, Fig. 8 c) highlights how the EDBM reached its target by producing (i) 1 M NaOH solution, used as the alkaline reactant for the MF-PFR, and (ii) 0.65 M HCl solution, sufficient for neutralization and cleaning purposes.

4.3. Energy performances of pilot units

Table 5 reports the energy consumption of each pilot plant, alongside the results of the specific energy performance indicators for the EDBM unit. As can be observed in Table 5, NF consumed 5.7 kW taking into account the energy consumed by the two high pressure pumps, the booster pump and the circulation pumps for the MMF and the outlet streams (NF permeate and retentate). 1.94 kW was calculated for the MF-PFR including the use of the drum filter. It is to be noted that of 1.94 kW, 0.98 was consumed by the main electrically-driven parts of the reactor (pumps), assuming that the auxiliaries (sensors and controllers) power consumption was 20 % of the total consumption of major items. On the other side, the remaining 0.96 kW of the drum filter were estimated considering (i) a utilization factor of 10 % and (ii) an auxiliaries power consumption equal to 20 % of the total consumption of the filter.

As regards the electrical energy consumption of the MED plant, 15.14 kW were consumed. However, it is worth mentioning that only 3.34 kW was really necessary for the operation of the plant, taking into account the energy consumed by (i) the circulation pumps of distillate and brine and (ii) the recycling pump of the brine stream. >50 % of the required power (8.2 kW) is used in the primary steam production from the waste heat produced by power plant.

The remaining 3.6 kW relates to the vacuum generator, that was an oversized liquid ring vacuum pump (chosen to speed up the start-up of the plant). As a matter of fact, it is to be noted that the liquid ring vacuum pump could have been substituted, for example, by a steam driven vacuum system, where the required steam could be potentially produced by recovering waste heat from the stack of the power plant.

As regards the specific electrical energy consumption (SEEC) of the MED pilot plant, the obtained SEEC value was, neglecting the primary steam production, in the range of 5–6 kWh/m^3. These values are consistent with other pilot plants with only 2 effects reported in literature [54,55]. However, lower values are possible for optimized industrial scale plants and are much closer to 2–3 kWh/m^3 (typical value for water production by seawater desalination), when proper pumps size and optimized configuration are possible.

As far as the EDBM is concerned, an energy consumption of 8.78 kW

Table 5
Energy performances of the pilot plants.

Technology	kW	Specific Energetic indicators	
NF	5.7		
MF-PFR	1.94	–	
EDBM	8.78	CE$_{HCl}$ [%]	50–70
		CE$_{NaOH}$ [%]	65–85
		SEC$_{HCl}$ [kWh/kg]	3.0–4.0
		SEC$_{NaOH}$ [kWh/kg]	2.0–3.0
MED	6.94	SEEC [kWh/m^3]	5.0–6.0

Table 6
Specific performances of the MED pilot plant.

MED specific performance indicators	
Gross GOR [−]	1.5–2.0
CF [−]	4.0–8.0

was registered for the EDBM unit. More specifically, such value was predominately related to the DC drive for the generation of the electric field in the EDBM stack, while a small portion of the power was required by circulation pumps (about 25 % of the total). Also in this case, the auxiliaries power consumption was assumed to be 20 % of the total energy consumed for the EDBM unit. Furthermore, the performance of the EDBM system could be evaluated in terms of current efficiency and specific energy consumption. Acid and base were produced with a current efficiency ranging between 50 and 70 % and 65–85 %, respectively. The lower current efficiency of the acid stream was due to the diffusion of the protons through the AEM towards the salt compartment. Due to this phenomenon, an acidified salt solution at the stack outlet was produced. A Specific energy consumption in the range of 3–4 and 2–3 kWh/kg was obtained for acid and base, respectively. The higher SEC of the acid was related to the lower CE recorded for this solution.

The obtained values of SEC were compared with values published in literature [56,57] for similar concentrations of chemicals. In the present case the salt solution has a significant lower concentration compared to those employed in previous studies (at least 1 M of NaCl).

4.4. Specific performances of the MED unit

To assess the performances of the MED pilot plant, further specific parameters were evaluated: (i) the concentration factor of NaCl and (ii) the GOR_{gross}. As it is possible to observe in Table 6, the concentration factor of NaCl reached a maximum value of 8. It is intended to specify that this result was obtained by producing a distillate with a conductivity lower than 30 μS/cm and without any scaling problems in the effects. As regards the GOR_{gross}, its value is linked to the number of effects of the MED unit. More precisely, as the number of effects increases, the amount of produced distillate increases, still relying on the single inlet steam at the first effect. In this specific case, the MED unit has 2 evaporative effects and the average GOR_{gross} value was comprised between 1.5 and 2.

4.5. Stability of pilot plants

As previously mentioned, the following paragraphs report the stability assessment of the main operating parameters of each technology during their daily operational run.

Moreover, the total amount of working hours for each technology of the treatment chain is reported as follows:

- Nano Filtration, total working hours 670;
- Multiple Feed Plug Flow Reactor, total working hours 480;
- Multi Effect Distillation, total working hours 70;
- Electro Dialysis with Bipolar Membrane, total working hours 880;
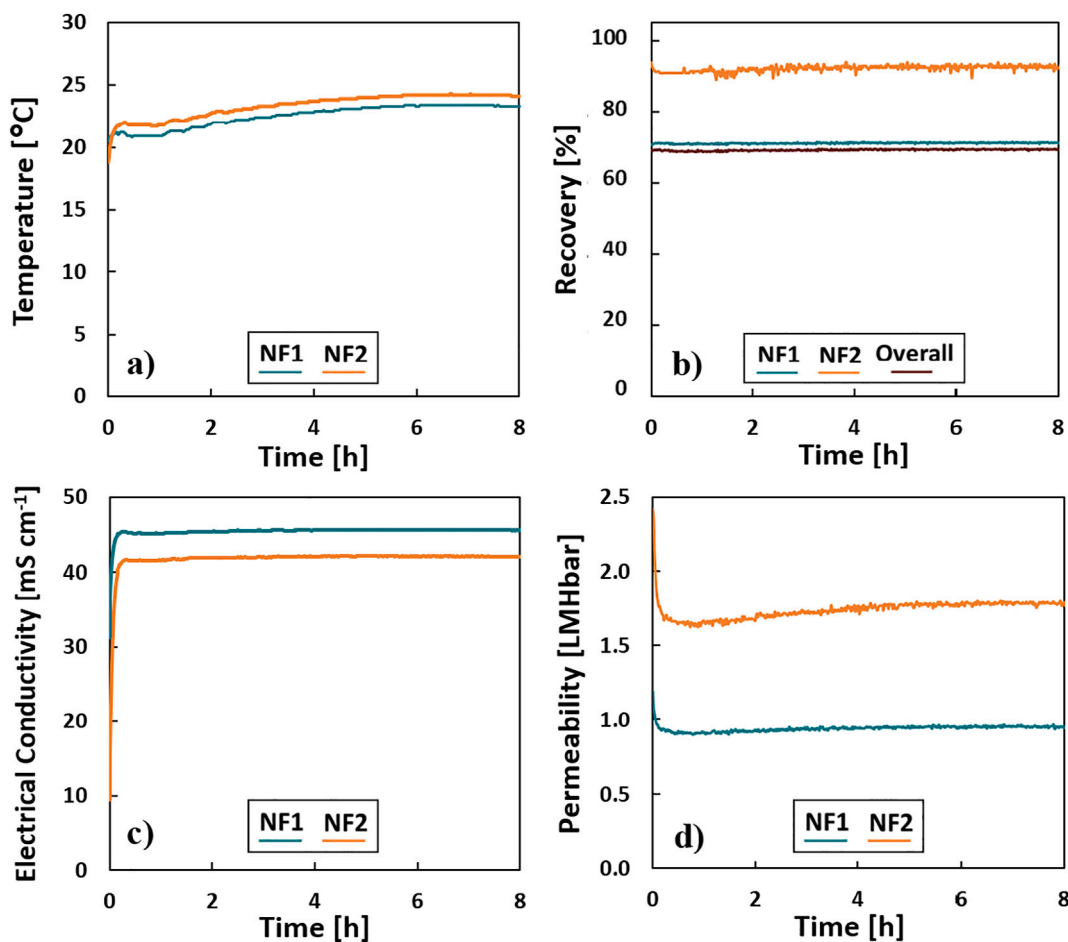- Evaporative ponds, total working hours 5090.

Fig. 9. a)The temperature of the feed streams, b) the permeate recovery, c) the electrical conductivity of NF1 and NF2 permeates, d) the membrane permeability of NF1, NF2 and/or the overall DPNF process, throughout the operation.

4.5.1. NF

To guarantee uniform feed conditions for the downstream units of the demo plant, the operational stability of the NF plant was assessed, monitoring the trend of four main parameters: Feed temperature (Fig. 9 a), NF pass recovery (Fig. 9 b), EC rejection (Fig. 9 c) and NF membrane permeability (Fig. 9 d). According to Fig. 9 a), the temperature of the seawater increased moderately throughout the operational run (8 h/ day). Nevertheless, the feed seawater conductivity was stable over time and presented an EC of 52 mS cm^{-1}. As far as the recovery of NF1 and NF2 are concerned, they were kept constant by the DPNF system at 71 % and 92 %, respectively, as can be seen in Fig. 9 b). Further demonstration of the stability of the NF process over time can be observed by the electrical conductivity EC for the NF1 permeate and NF2 permeate (see Fig. 9c). More specifically, whilst the EC of NF1 permeate was 45.3 mS/ cm over the entire operational run, the EC of NF2 permeate reached a lower value of 41.6 mS/cm. Such difference was due to the lower feed concentration of NF2.

As for the membrane permeability of NF1 and NF2, a trend somewhat similar to that of the feed temperature was observed in Fig. 9 d). When the temperature increased, the membranes were more permeable and less pressure was required to produce a fixed amount of permeate. Hence, the membrane permeability increased when the temperature of the seawater increased (during the day). Furthermore, the membrane permeability of NF2 was higher than the membrane permeability of NF1. The difference in membrane permeability was related to the amount of ions that were rejected by the membranes in the two passes. When compared to NF2, NF1 rejected ions from a stream that had a higher multivalent ion concentration, experiencing a higher osmotic pressure difference between the feed/concentrate and permeate side of the membranes. Therefore, to overcome the respective osmotic pressure difference to produce permeate, a higher applied pressure was necessary. All in all, the DPNF operated stably, based on the steady trend of the permeate recovery throughout the operation.

4.5.2. MF-PFR

As mentioned in Section 3.2, the MF-PFR operated in two consecutive precipitation steps for Mg(OH)$_2$ and Ca(OH)$_2$ recovery, respectively. During the operation of each step (8 h/day for the 1st step and 5 h/day for the 2nd step), relevant operative parameters (pH and brine and alkaline flow rates) were recorded and plotted against time in order to assess the stability of the system. To be noted that the stability of pH and flow rates would consequently provide a constant recovery and purity of the hydroxides.

Fig. 10 reports the variation of such parameters in time for the magnesium precipitation step (Fig. 10 a) and for the calcium precipitation step (Fig. 10 b). As illustrated in Fig. 10 a) and b), the outlet reaction pH and brine flow-rate, in both precipitation steps, were stable during the experiments. Stability could have been compromised by pressure drops caused by nozzle scaling or slight variation in the magnesium (or calcium) content of the inlet brine. It is the latter that explains the slight increase of the alkaline flow rate in time. However, the implemented control system was appropriately developed to minimize these disturbance effects and successfully accomplished such task.

4.5.3. EDBM

To ensure (i) the continuous supply of a target 1 M NaOH solution to the MF-PFR and (ii) the production of a HCl solution (with a concentration varying in a narrow range), it was also crucial to investigate the stability of the EDBM pilot plant. The main parameters that were assessed in time were: (i) the concentration of HCl and NaOH (Fig. 11 a), (ii) the required applied voltage of the pilot system (Fig. 11 b), (iii) the calculated specific energy consumption referred to HCl and NaOH (Fig. 11 c) and (iv) the current efficiency of the system referred to HCl and NaOH (Fig. 11 d). As can be observed in Fig. 11 a), the concentration of NaOH and HCl were maintained constant at 1 mol/L and 0.65 mol/L, respectively. Stability was guaranteed thanks to the advanced controlled system implemented [43]. Furthermore, the reason of the lower HCl concentration was most likely due to (i) the phenomenon of diffusion and loss of proton ions into the salt and alkaline compartments and (ii) the slight increase in outlet acid solution flowrate due to osmotic and electroosmotic water flux [41]. The resulting voltage of the EDBM stack fluctuated with small deviations around 55 V, as illustrated in Fig. 11 b). Finally, as a consequence of the stable behavior of the system, the stability of the calculated SEC and CE was guaranteed during the operational run (see Fig. 11 c and d).

4.5.4. MED

To assess the potential for fresh water production and recovery of NaCl, which is eventually collected in the downstream evaporation ponds, it was also important to evaluate the operational stability of the MED pilot plant. To such end, the trend of the operating temperature and pressure of the 1st effect were monitored during an operational run of 4 h. As can be observed in Fig. 12 a), after the first hour of start-up phase of the plant, both the pressure and temperature were fairly constant around a value of 50 °C and 0.1 bar, respectively. This result was of significant importance since the MED pilot operated, exploiting waste heat from the diesel engines of the local Lampedusa Power Plant, which is often characterized by slight and unpredictable variations of its available temperature. As far as the quality of the two outlet streams is concerned, the brine and distillate conductivity were monitored during a daily operational run, maintaining constant values around 195 mS cm^{-1} and 20 μS cm^{-1}, respectively (see Fig. 12 b). Thus, two main goals were successfully achieved: (i) high quality water production and (ii) maximized NaCl recovery.
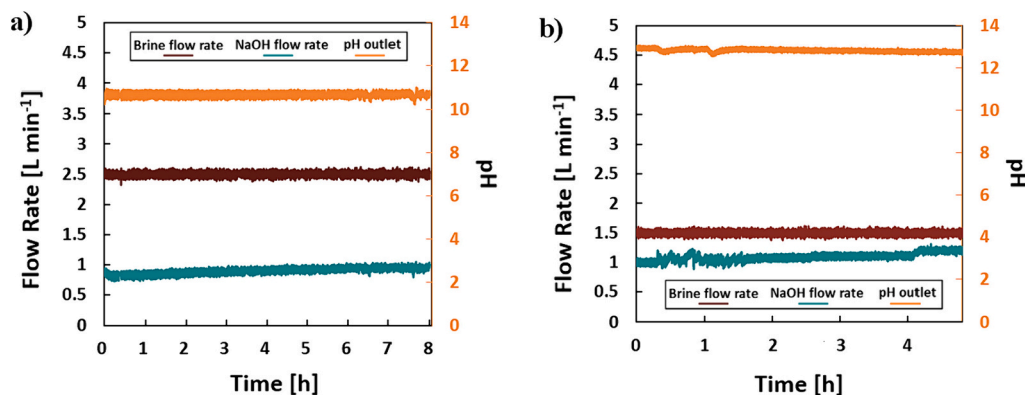

Fig. 10. Variation of pH and both flow rates during the operational run of a) the first precipitation step for Mg(OH)$_2$ production and b) the second precipitation step for Ca(OH)$_2$ production.
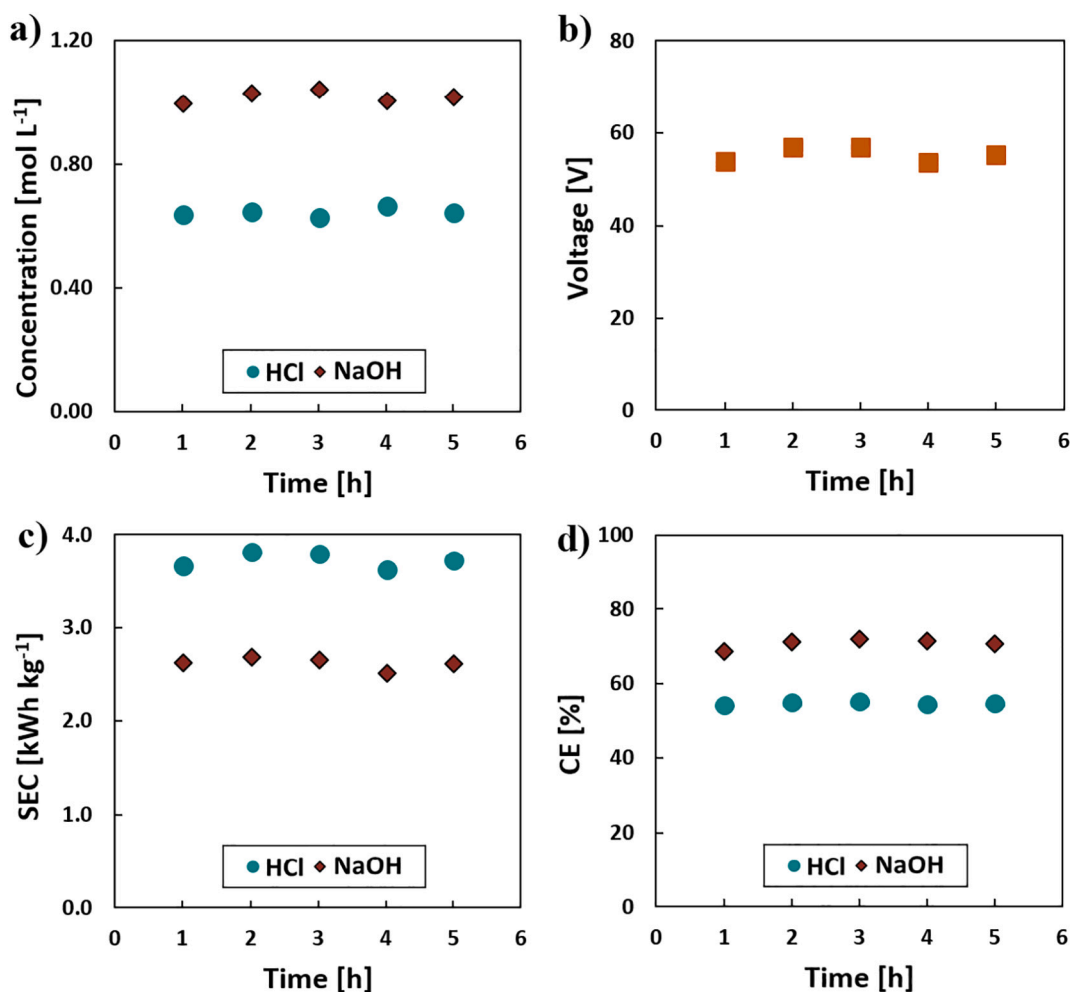
Fig. 11. a) trend of HCl and NaOH concentration, b) trend of voltage, c) trend of Specific Energy consumption referred to HCl and NaOH produced, d) trend of current efficiency referred to HCl and NaOH during operation.
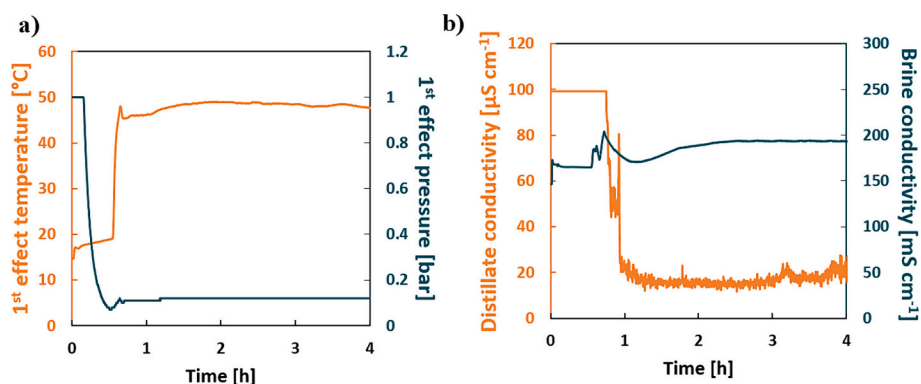

Fig. 12. a) trend of 1st effect operating temperature and pressure in time; b) trend of distillate and brine conductivity in time.

4.6. Integration and circularity assessment

The integration and circularity assessment of the pilot plant provides invaluable insights for guiding future decisions and strategies. In this assessment, a full integration of the units was assumed. This meant that the capacity of the five different technologies perfectly match each other, eliminating discharge issues experienced in real pilot units due to practical constraints within the project.

Fig. 13 presents a detailed mass balance of the full integrated system

in a Sankey diagram. The Sankey diagram prominently illustrates the efficient recovery of valuable resources within the fully integrated system. For instance, it reveals a closed-loop system where chemicals, such as NaOH and HCl, can be recirculated within the system (in MF-PFR) for the precipitation of $Mg(OH)_2$ and $Ca(OH)_2$. Fig. 13 provides clear evidence of significant waste reduction compared to linear desalination systems. In the fully integrated system, waste streams are minimized, and many materials are efficiently recycled and repurposed, as demonstrated by the loops and connections in the diagram.
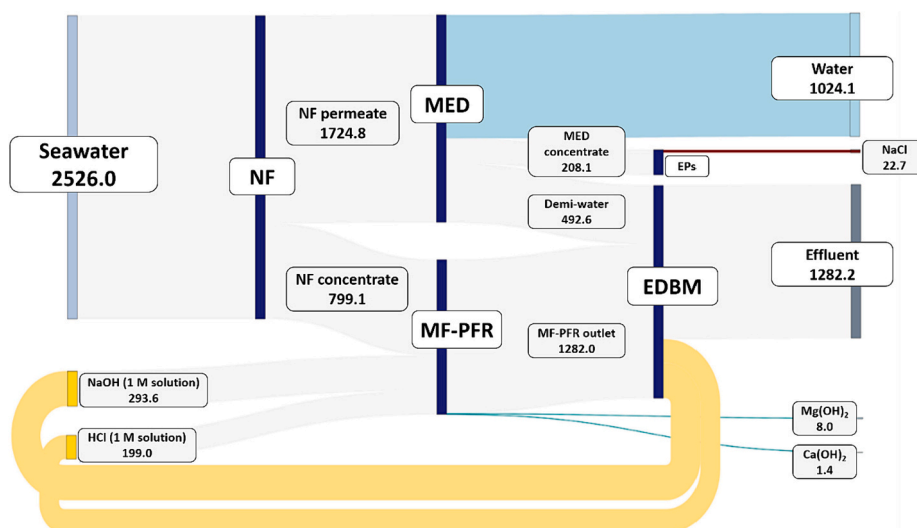
Fig. 13. Mass balance [kg/h] of a fully integrated system. The recovered chemicals, NaOH and HCl, are recirculated in the system (MF-PFR). Saline effluent from the EDBM can be recycled back to the system (MED).

Table 7
Circularity assessment results.

Indicator	Percentage
Total brine reduction (TBR)	92.7 %
Resource Efficiency (RE)	
Water	79.7 %
Mg(OH)$_2$	90–100 %
Ca(OH)$_2$	50–80 %
NaCl	>95 %
HCl	90–95 %
NaOH	90–95 %
Circular Chemical Inflow (CCI)	100 %
Energy Self-Sufficiency (ESS)	85.4 %

Table 7 summarizes the integration and circularity assessment results. The analysis indicated a remarkable total brine reduction of 92.7 %. This substantial reduction in brine waste, compared to conventional linear desalination methods, was a significant achievement. It underscored the potential for environmental improvement, demonstrating effective resource recovery from seawater brine.

In assessing RE, the results revealed a notably high recovery of all valuable materials that would be discharged back to the environment in linear systems. A particular remark for the recovery of water, which indicates the system's advantage in terms of water availability when compared to linear systems. This underscored the potential for more sustainable resource management, as the pilot plant system excelled in efficiently recovering valuable materials and reducing waste compared to conventional linear processes.

The circularity assessment also revealed a CCI of 100 %. This meant that all chemicals, such as HCl and NaOH, required for the process were internally produced from seawater brine. This result was a noteworthy step towards (i) reducing reliance on external sources and (ii) securing the supply chain for critical materials like magnesium.

The high energy requirements of the system represented a challenge. However, there were opportunities for mitigating this risk. Integrating the power station with the desalination plant could enhance the water-energy nexus, potentially reducing energy consumption and costs. Additionally, the energy gain from utilizing waste heat to meet thermal energy requirements could significantly boost the system's overall energy self-sufficiency.

Circular economy is not the responsibility of a single player. This means that a multitude of stakeholders are involved in ensuring a continuous material stream that flows back into the value chain.

This work can serve as a starting point for cross-value-chain conversations, particularly in the context of seawater mining. Engaging with various stakeholders, including suppliers, manufacturers, and policymakers, is essential for realizing the full potential of circularity in resource management.

Overall, the impact of the results is evident in the practical advancements achieved, from substantial waste reduction to the establishment of a ZLD system and the potential for marketable salt and chemical production from integrated desalination and brine treatment plants. These findings not only contribute to the scientific understanding of integrated desalination systems but also pave the way for transformative changes in environmental sustainability.

Regarding the environmental aspect, the proposed system significantly reduces the environmental impact on the marine ecosystem compared to conventional desalination due to the brine discharge elimination. Additionally, the achieved high energy self-sufficiency holds promise as a potential solution for energy-scarce regions, such as Lampedusa.

Therefore, this work stands as a catalyst for progressive change, providing a foundation for future discussions and actions in resource management.

5. Conclusions

Within the context of sustainable minerals production, the scientific community has recently focused much attention on the proposal of MLD/ZLD schemes treating seawater/brine, as a solution to both (a) land mining depletion and (b) the negative environmental impact of seawater desalination processes. However, many suggested schemes are still limited to concept proposals or lab-scale implementation. For the first time in literature, this work presents the results of a large-scale demonstrative plant for seawater valorisation (feed capacity of 2.46 m^3/h), capable of recovering several valuable resources and exploiting waste heat from the cooling circuits of diesel engine of a small island (Lampedusa) Power Plant. The seawater treatment chain comprised 5 different technologies: (i) Nanofiltration, (ii) Multiple Feed – Plug Flow Reactor, (iii) ElectroDialysis with Bipolar Membranes, (iv) Multi-Effect Distillation and (v) Evaporation Ponds. Results showed that:

(i) High rejection of bivalent ions, such as magnesium, calcium and sulphate was obtained by the NF unit, highlighting the capability of the unit to produce a retentate very rich in magnesium and calcium;

(ii) three valuable resources: $Mg(OH)_2$ (purity: 90–98 %), $Ca(OH)_2$ and NaCl (purity >99 %);

(iii) high concentrate brine, along with high quality freshwater (recovery up to 85 % and high grade quality freshwater (conductivity <30 μS/cm)) were produced by the MED, obtaining a concentration factor up to 7;

(iv) two chemicals were produced by EDBM unit and internally used as reactants for the precipitation of magnesium and/or calcium in form of hydroxides and for cleaning/neutralizing purposes within the treatment chain (1 M NaOH and 0.65 M HCl solutions);

(v) high grade quality of sodium chloride (purity close to 100 %) was produced by the evaporation ponds using the concentrated brine produced by the MED.

Furthermore, the stability of each unit during the daily operational run was assessed and successfully achieved, demonstrating not only the technical feasibility of the proposed demo plant, but also the feasibility of MLD as a sustainable alternative for minerals recovery.

Finally, a theoretical circularity assessment analysis highlighted how the system can potentially be operated under a fully circular mode, with zero chemicals input from outside and extremely high recovery rates for water and chemicals generated in the process.

CRediT authorship contribution statement

C. Morgante: Conceptualization, Data curation, Formal analysis, Investigation, Methodology, Writing – original draft. **F. Vassallo:** Conceptualization, Data curation, Formal analysis, Investigation, Methodology, Writing – original draft. **C. Cassaro:** Conceptualization, Data curation, Formal analysis, Investigation, Methodology, Writing – original draft. **G. Virruso:** Conceptualization, Data curation, Formal analysis, Investigation, Methodology, Writing – original draft. **D. Diamantidou:** Data curation, Formal analysis, Methodology, Writing – original draft. **N. Van Linden:** Data curation, Formal analysis, Methodology, Writing – review & editing. **A. Trezzi:** Data curation, Formal analysis, Methodology, Supervision, Writing – review & editing. **C. Xenogianni:** Formal analysis, Methodology, Writing – review & editing. **R. Ktori:** Conceptualization, Data curation, Formal analysis, Methodology, Writing – original draft. **M. Rodriguez:** Conceptualization, Data curation, Formal analysis, Investigation, Methodology, Supervision. **G. Scelfo:** Data curation, Formal analysis, Investigation, Writing – original draft. **S. Randazzo:** Data curation, Formal analysis, Methodology, Writing – original draft. **A. Tamburini:** Conceptualization, Formal analysis, Methodology, Supervision, Validation, Writing – review & editing. **A. Cipollina:** Conceptualization, Formal analysis, Funding acquisition, Investigation, Methodology, Supervision, Writing – review & editing. **G. Micale:** Conceptualization, Formal analysis, Funding acquisition, Methodology, Project administration, Resources, Supervision, Writing – review & editing. **D. Xevgenos:** Conceptualization, Formal analysis, Funding acquisition, Methodology, Project administration, Resources, Supervision, Writing – review & editing.

Declaration of competing interest

The authors declare that they have no known competing financial interests or personal relationships that could have appeared to influence the work reported in this paper.

Data availability

Data will be made available on request.

Acknowledgments

References

[1] A.Y. Hoekstra, Water scarcity challenges to business, Nat. Clim. Chang. 4 (2014) 318–320, https://doi.org/10.1038/nclimate2214.

[2] A. Panagopoulos, A comparative study on minimum and actual energy consumption for the treatment of desalination brine, Energy 212 (2020) 118733, https://doi.org/10.1016/j.energy.2020.118733.

[3] M.N. Soliman, F.Z. Guen, S.A. Ahmed, H. Saleem, M.J. Khalil, S.J. Zaidi, Energy consumption and environmental impact assessment of desalination plants and brine disposal strategies, Process. Saf. Environ. Prot. 147 (2021) 589–608, https://doi.org/10.1016/j.psep.2020.12.038.

[4] E. Jones, M. Qadir, M.T.H. van Vliet, V. Smakhtin, S. mu Kang, The state of desalination and brine production: a global outlook, Sci. Total Environ. 657 (2019) 1343–1356, https://doi.org/10.1016/j.scitotenv.2018.12.076.

[5] T. Peters, D. Pintó, Seawater intake and pre-treatment/brine discharge - environmental issues, Desalination 221 (2008) 576–584, https://doi.org/10.1016/j.desal.2007.04.066.

[6] F. Macedonio, E. Curcio, E. Drioli, Integrated membrane systems for seawater desalination: energetic and exergetic analysis, economic evaluation, experimental study, Desalination 203 (2007) 260–276, https://doi.org/10.1016/j.desal.2006.02.021.

[7] M.O. Mavukkandy, C.M. Chabib, I. Mustafa, A. Al Ghaferi, F. AlMarzooqi, Brine management in desalination industry: from waste to resources generation, Desalination 472 (2019) 114187, https://doi.org/10.1016/j.desal.2019.114187.

[8] Z. Wang, A. Deshmukh, Y. Du, M. Elimelech, Minimal and zero liquid discharge with reverse osmosis using low-salt-rejection membranes, Water Res. 170 (2020) 115317, https://doi.org/10.1016/j.watres.2019.115317.

[9] P. Loganathan, G. Naidu, S. Vigneswaran, Mining valuable minerals from seawater: a critical review, Environ. Sci. Water Res. Technol. 3 (2017) 37–53, https://doi.org/10.1039/c6ew00 268d.

[10] C.A. Quist-Jensen, F. Macedonio, E. Drioli, Membrane crystallization for salts recovery from brine—an experimental and theoretical analysis, Desalin. Water Treat. 57 (2016) 7593–7603, https://doi.org/10.1080/19443994.2015.1030110.

[11] S. Yang, F. Zhang, H. Ding, P. He, H. Zhou, Lithium metal extraction from seawater, Joule 2 (2018) 1648–1651, https://doi.org/10.1016/j.joule.2018.07.006.

[12] B.A. Sharkh, A.A. Al-Amoudi, M. Farooque, C.M. Fellows, S. Ihm, S. Lee, S. Li, N. Voutchkov, Seawater desalination concentrate—a new frontier for sustainable mining of valuable minerals, Npj Clean Water 5 (2022) 1–16, https://doi.org/10.1038/s41545-022-00153-6.

[13] S. van Wyk, S.O. Odu, A.G.J. van der Ham, S.R.A. Kersten, Design and results of a first generation pilot plant for supercritical water desalination (SCWD), Desalination 439 (2018) 80–92, https://doi.org/10.1016/j.desal.2018.03.028.

[14] S. van Wyk, A.G.J. van der Ham, S.R.A. Kersten, Potential of supercritical water desalination (SCWD) as zero liquid discharge (ZLD) technology, Desalination 495 (2020) 114593, https://doi.org/10.1016/j.desal.2020.114593.

[15] A. Panagopoulos, Beneficiation of saline effluents from seawater desalination plants: fostering the zero liquid discharge (ZLD) approach - a techno-economic evaluation, J. Environ. Chem. Eng. 9 (2021), https://doi.org/10.1016/j.jece.2021.105338.

[16] A. Panagopoulos, Energetic, economic and environmental assessment of zero liquid discharge (ZLD) brackish water and seawater desalination systems, Energy Convers. Manag. Comp. Techno-Economic Environ. Anal. Minimal Liq. Disch. Zero Liq. Disch. Desalin. Syst. Seawa. 235 (2021), https://doi.org/10.1016/j.enconman.2021.113957.

[17] A. Panagopoulos, V. Giannika, Comparative techno-economic and environmental analysis of minimal liquid discharge (MLD) and zero liquid discharge (ZLD) desalination systems for seawater brine treatment and valorization, Sustain. Energy Technol. Assess. 53 (2022), https://doi.org/10.1016/j.seta.2022.102477.

[18] A. Panagopoulos, Techno-economic assessment and feasibility study of a zero liquid discharge (ZLD) desalination hybrid system in the eastern Mediterranean, Chem. Eng. Process. - Process Intensif. 178 (2022), https://doi.org/10.1016/j.cep.2022.109029.

[19] A. Panagopoulos, Techno-economic assessment of zero liquid discharge (ZLD) systems for sustainable treatment, minimization and valorization of seawater brine, J. Environ. Manage. 306 (2022), https://doi.org/10.1016/j.jenvman.2022.114488.

[20] C. Morgante, F. Vassallo, D. Xevgenos, A. Cipollina, M. Micari, A. Tamburini, G. Micale, Valorisation of SWRO brines in a remote island through a circular approach: techno-economic analysis and perspectives, Desalination 542 (2022), https://doi.org/10.1016/j. desal.2022.116005.

[21] E. El-Zanati, K.M. El-Khatib, Integrated membrane -based desalination system, Desalination 205 (2007) 15–25, https://doi.org/10.1016/j.desal.2006.03.548.

[22] F. Tahir, S.G. Al-Ghamdi, Integrated MED and HDH desalination systems for an energy-efficient zero liquid discharge (ZLD) system, Energy Rep. 8 (2022) 29–34, https://doi.org/10.1016/j.egyr.2022.01.028.

[23] K. Poirier, N. Al Mhanna, K. Patchigolla, Techno-economic analysis of brine treatment by multi-crystallization separation process for zero liquid discharge, Separations 9 (2022), https://doi.org/10.3390/separations9100295.

[24] G. Al Bazedi, R.S. Ettouney, S.R. Tewfik, M.H. Sorour, M.A. El-Rifai, Salt recovery from brine generated by large-scale seawater desalination plants, Desalin. Water Treat. 52 (2014) 4689–4697, https://doi.org/10.1080/19443994.2013.810381.

[25] M. Kieselbach, T. Hogen, S.U. Geißen, T. Track, D. Becker, H.J. Rapp, J. Koschikowski, J. Went, H. Horn, F. Saravia, A. Bauer, R. Schwantes, D. Pfeifle, N. Heyn, M. Weissroth, B. Fitzke, Brines from industrial water recycling: new ways to resource recovery, J. Water Reuse Desalin. 10 (2020) 443–461, https://doi.org/10.2166/wrd.2020. 033.

[26] D. von Eiff, P.W. Wong, Y. Gao, S. Jeong, A.K. An, Technical and economic analysis of an advanced multi-stage flash crystallizer for the treatment of concentrated brine, Desalination 503 (2021) 114925, https://doi.org/10.1016/j.desal.2020.114925.

[27] R. Ashu, E. Curcio, E. Brauns, W. Van Baak, E. Fontananova, G. Di, Membrane distillation and reverse Electrodialysis for near-zero liquid discharge and low energy seawater desalination, J. Membr. Sci. 496 (2015) 325–333, https://doi.org/10.1016/j. memsci.2015.09.008.

[28] W. Zhang, M. Miao, J. Pan, A. Sotto, J. Shen, C. Gao, B. Van Der Bruggen, Process economic evaluation of resource valorization of seawater concentrate by membrane technology, ACS Sustain. Chem. Eng. 5 (2017) 5820–5830, https://doi.org/10.1021/acssus-chemeng.7b00555.

[29] X. Ji, E. Curcio, S. Al Obaidani, G. Di Profio, E. Fontananova, E. Drioli, Membrane distillation-crystallization of seawater reverse osmosis brines, Sep. Purif. Technol. 71 (2010) 76–82, https://doi.org/10.1016/j.seppur.2009.11.004.

[30] D. Xevgenos, P. Michailidis, K. Dimopoulos, M. Krokida, M. Loizidou, Design of an innovative vacuum evaporator system for brine concentration assisted by software tool simulation, Desalin. Water Treat. 53 (2015) 3407–3417, https://doi.org/10.1080/19443994.2014.948660.

[31] D. Xevgenos, A. Vidalis, K. Moustakas, D. Malamis, M. Loizidou, Sustainable management of brine effluent from desalination plants: the SOL-BRINE system, Desalin. Water Treat. 53 (2015) 3151–3160, https://doi.org/10.1080/19443994.2014.933621.

[32] D. Xevgenos, K. Moustakas, D. Malamis, M. Loizidou, An overview on desalination & sustainability: renewable energy-driven desalination and brine management, Desalin. Water Treat. 57 (2016) 2304–2314, https://doi.org/10.1080/19443994.2014.984927.

[33] A.S. Al-Amoudi, S. Ihm, A.M. Farooque, E.S.B. Al-Waznani, N. Voutchkov, Dual brine concentration for the beneficial use of two concentrate streams from desalination plant - concept proposal and pilot plant demonstration, Desalination 564 (2023) 116789, https://doi.org/10.1016/j.desal.2023.116789.

[34] Proposal-Water Mining Horizon 2020, 2020, 2020.

[35] A. Culcasi, R. Ktori, A. Pellegrino, M. Rodriguez-pascual, M.C.M. Van Loosdrecht, Towards sustainable production of minerals and chemicals through seawater brine treatment using eutectic freeze crystallization and Electrodialysis with bipolar membranes, J. Clean. Prod. 368 (2022), https://doi.org/10.1016/j.jclepro.2022.133143.

[36] L.F. Petrik, H.H. Ngo, Voices From wastewater to resource, One Earth 5 (2022) 122–125, https://doi.org/10.1016/j.oneear.2022.01.011.

[37] C. Morgante, X. Ma, X. Chen, D. Wang, V. Boffa, V. Stathopoulos, J. Lopez, J. L. Cortina, A. Cipollina, A. Tamburini, G. Micale, Metal-organic-framework-based nanofiltration membranes for selective multi-cationic recovery from seawater and brines, J. Membr. Sci. 685 (2023), https://doi.org/10.1016/j.memsci.2023.121941.

[38] M. Bevacqua, F. Vassallo, A. Cipollina, G. Micale, A. Tamburini, M. Papapetrou, F. Vicari, Reattore e processo di precipitazione di un prodotto solido, Patent Application Number IT102021000012473, 2021.

[39] F. Vassallo, D. La Corte, N. Cancilla, A. Tamburini, M. Bevacqua, A. Cipollina, G. Micale, A pilot-plant for the selective recovery of magnesium and calcium from waste brines, Desalination 517 (2021) 115231, https://doi.org/10.1016/j.desal.2021.115231.

[40] C. Morgante, F. Vassallo, G. Battaglia, A. Cipollina, F. Vicari, A. Tamburini, G. Micale, Influence of operational strategies for the recovery of magnesium

hydroxide from brines at a pilot scale, Ind. Eng. Chem. Res. (2022), https://doi.org/10.1021/acs.iecr.2c0 2935.

[41] T. León, S. Abdullah Shah, J. López, A. Culcasi, L. Jofre, A. Cipollina, J.L. Cortina, A. Tamburini, G. Micale, Electrodialysis with bipolar membranes for the generation of NaOH and HCl solutions from brines: an inter-laboratory evaluation of thin and ultrathin non-woven cloth-based ion-exchange membranes, Membranes (Basel) 12 (2022), https://doi.org/10.3390/membranes12121204.

[42] A. Culcasi, L. Gurreri, A. Cipollina, A. Tamburini, G. Micale, A comprehensive multi-scale model for bipolar membrane electrodialysis (BMED), Chem. Eng. J. 437 (2022), https://doi.org/10.1016/j.cej.2022.135317.

[43] C. Cassaro, G. Virruso, A. Culcasi, A. Cipollina, A. Tamburini, G. Micale, Electro-dialysis with bipolar membranes for the sustainable production of chemicals from seawater brines at pilot plant scale, ACS Sustain. Chem. Eng. 11 (2023) 2989–3000, https://doi.org/10.1021/acssuschemeng.2c06636.

[44] M. Al-Shammiri, M. Safar, Multi-effect distillation plants: state of the art, Desalination 126 (1999) 45–59, https://doi.org/10.1016/S0011-9164(99)00154-X.

[45] M. Micari, M. Moser, A. Cipollina, B. Fuchs, B. Ortega-Delgado, A. Tamburini, G. Micale, Techno-economic assessment of multi-effect distillation process for the treatment and recycling of ion exchange resin spent brines, Desalination 456 (2019) 38–52, https://doi.org/10.1016/j.desal.2019.01.011.

[46] D.G. Akridge, Methods for calculating brine evaporation rates during salt production, J. Archaeol. Sci. 35 (2008) 1453–1462, https://doi.org/10.1016/j.jas.2007.10.013.

[47] F. Vicari, S. Randazzo, J. López, M. Fernández de Labastida, V. Vallès, G. Micale, A. Tamburini, G. D'Alì Staiti, J.L. Cortina, A. Cipollina, Mining minerals and critical raw materials from bittern: understanding metal ions fate in saltwork ponds, Sci. Total Environ. 847 (2022), https://doi.org/10.1016/j.scitotenv.2022.157544.

[48] ENEA, ENEA. www.solaritaly.enea.it.pdf, 2023 (n.d.).

[49] C.E. Nika, V. Vasilaki, A. Expósito, E. Katsou, Water cycle and circular economy: developing a circularity assessment framework for complex water systems, Water Res. 187 (2020), https://doi.org/10.1016/j.watres.2020.116423.

[50] K. Park, G.E.O. Kremer, Text mining-based categorization and user perspective analysis of environmental sustainability indicators for manufacturing and service systems, Ecol. Indic. 72 (2017) 803–820, https://doi.org/10.1016/j.ecolind.2016.08.027.

[51] C.E. Nika, V. Vasilaki, D. Renfrew, M. Danishvar, A. Echchelh, E. Katsou, Assessing circularity of multi-sectoral systems under the water-energy-food-ecosystems (WEFE) nexus, Water Res. 221 (2022), https://doi.org/10.1016/j.watres.2022.118842.

[52] F. Vassallo, D. La Corte, A. Cipollina, A. Tamburini, G. Micale, High purity recovery of magnesium and calcium hydroxides from waste brines, Chem. Eng. Trans. 86 (2021) 931–936, https://doi.org/10.3303/CET2186156.

[53] Codex Alimentarius Commission, Codex Standard for Food Grade Salt, 2006.

[54] D. Zhao, J. Xue, S. Li, H. Sun, Q. Zhang, Theoretical analyses of thermal and economical aspects of multi-effect distillation desalination dealing with high-salinity wastewater, Desalination 273 (2011) 292–298, https://doi.org/10.1016/j.desal.2011.01.048.

[55] S. Aly, H. Manzoor, S. Simson, A. Abotaleb, J. Lawler, A.N. Mabrouk, Pilot testing of a novel multi effect distillation (MED) technology for seawater desalination, Desalination 519 (2022) 115221, https://doi.org/10.1016/j.desal.2021.115221.

[56] V. Mavrov, H. Chmiel, B. Heitele, F. Rögener, Desalination of surface water to industrial water with lower impact on the environment part 4: treatment of effluents from water desalination stages for reuse and balance of the new technological concept for water desalination, Desalination 124 (1999) 205–216, https://doi.org/10.1016/S0011-9164(99)00105-8.

[57] M. Reig, S. Casas, C. Valderrama, O. Gibert, J.L. Cortina, Integration of monopolar and bipolar electrodialysis for valorization of seawater reverse osmosis desalination brines: production of strong acid and base, Desalination 398 (2016) 87–97, https://doi.org/10.1016/j.desal.2016.07.024.